

# PARAMETER IDENTIFICATION OF THE STICS CROP MODEL, USING AN ACCELERATED FORMAL MCMC APPROACH

Dumont B.<sup>1\*</sup>, Leemans V.<sup>1</sup>, Mansouri M.<sup>1</sup>, Bodson B.<sup>2</sup>, Destain J.-P.<sup>3</sup>, Destain M.-F.<sup>1</sup>

<sup>1</sup>, ULg (GxABT), Unité de Mécanique et construction

<sup>2</sup>, ULg (GxABT), Unité de Phytotechnie des régions tempérées

<sup>3</sup>, ULg (GxABT), Centre wallon de Recherches agronomiques (CRA-W)

\* Corresponding author: 2 Passage des Déportés, 5030 Gembloux, Belgium

@: [benjamin.dumont@ulg.ac.be](mailto:benjamin.dumont@ulg.ac.be)

Tel.: +32(0)81/62.21.63, fax: +32(0)81/62.21.67

**Keywords:** Crop model – Parameter estimation – Bayes – STICS – DREAM

## Abstract

This study presents a Bayesian approach for the parameters' identification of the STICS crop model based on the recently developed Differential Evolution Adaptive Metropolis (DREAM) algorithm. The posterior distributions of nine specific crop parameters of the STICS model were sampled with the aim to improve the growth simulations of a winter wheat (*Triticum aestivum* L.) culture. The results obtained with the DREAM algorithm were initially compared to those obtained with a Nelder-Mead Simplex algorithm embedded within the OptimISTICS package. Then, three types of likelihood functions implemented within the DREAM algorithm were compared, namely the standard least square, the weighted least square, and a transformed likelihood function that makes explicit use of the coefficient of variation (CV). The results showed that the proposed CV likelihood function allowed taking into account both noise on measurements and heteroscedasticity which are regularly encountered in crop modelling.

## 26 **1. Introduction**

27           In recent decades, the number of dynamic crop models developed for estimating crop  
28 performance based on the interactions between environment and agricultural management has greatly  
29 increased. There are two types of models: specific and generic. The former are process-oriented  
30 models capable of simulating water balance, nitrogen balance, growth and the development of a given  
31 crop, while maintaining reasonable input requirements. For example, the CERES-Wheat model  
32 simulates the growth, development and yield of wheat (*Triticum aestivum* L.), taking account of the  
33 effects of weather, genetics, soil (water, carbon and nitrogen), planting, irrigation and nitrogen  
34 fertilizer management (Ritchie and Otter, 1984; Singh et al., 2008). Generic models are based on  
35 physiological principles for growth and development processes that are common across many crops.  
36 They use a modular code for crop modelling, providing easy ways of comparing modelling approaches  
37 without the need to change the code. They also provide a way to interpret data from field experiments  
38 in various environments (Monteith, 1996) and to analyse the processes at the plant component level  
39 (Confalonieri and Bechini, 2004). Well-known generic models that are able to simulate the growth and  
40 development of various crops (wheat, maize, sorghum, etc.) are EPIC (William et al., 1989),  
41 WOFOST (Van Diepen et al., 1989), DAISY (Hansen et al., 1990), STICS (Brisson et al., 1998) and  
42 SALUS (Basso and Ritchie, 2005).

43           The number of parameters required by generic models is higher than for specific models. The  
44 STICS model used in this study (Brisson et al., 1998; Brisson et al., 2003; Brisson et al., 2009) is  
45 characterized by its ability to adapt to a wide range of agro-environmental issues and its adaptability to  
46 various crops : e.g. wheat, sugarbeet, sugarcane, rice. It implies that the number of parameters  
47 involved is high: more than 200 parameters are arranged in three main groups related to (i) soil, (ii)  
48 plant characteristics (species or genotype) and (iii) management techniques. The soil properties can be  
49 determined from pedotransfer functions but these give the mean soil properties for rather broadly  
50 defined soil textures classes and therefore provide limited site-specific information (Wösten et al.,  
51 1999). The soil properties can also be measured directly on site, but this is very costly and time  
52 consuming. Management techniques are usually known as they reflect the farmer's decisions. The

53 parameters related to plant growth and development are determined from the literature, from  
54 experiments conducted on specific processes included in the model (*e.g.* mineralization rate, critical  
55 nitrogen dilution curve) or from calibrations based on large experimental databases (Launay et al.,  
56 2005; Flenet et al., 2004). In all cases, the propagation of uncertainty about the parameters could lead  
57 to a model that does not accurately describe responses observed in the field.

58 Parameter estimation is not straightforward in generic crop models. Most of the equations are  
59 non-linear, coupled and hierarchical; the number of parameters to optimize is important; and field  
60 spatial variability and climatic temporal fluctuations are high. Several methods have been proposed for  
61 parameter estimation, based on frequentist or Bayesian approaches (Beven, 1989; Wallach et al.  
62 2006). In the first category are sensitivity analyses (Wallach et al., 2001; Ruget et al., 2002; Bechini et  
63 al., 2006; Makowski et al., 2006; Monod et al., 2006; Campolongo et al., 2007; Lamboni et al., 2009)  
64 and stepwise regression methods (Wallach et al., 2001, 2006). Recently, Wallach et al. (2009, 2011)  
65 developed a software package suited to the STICS crop model (OptimiSTICS) that used the Extended  
66 Fast algorithm (also used by Varella et al., 2010a, 2011) to analyse the sensitivity indices.

67 The Bayesian approaches (Gilks et al., 1996; Jansen and Hagennars, 2004 ; Makowski et al.  
68 2002) are becoming increasingly popular for estimating model outputs and parameters distributions in  
69 different types of complex models, like the simulation of biological processes (Minunno et al., 2013),  
70 environmental (Dietzel and Reichert, 2012; Rasmussen and Hamilton, 2012), hydrological (Jeremiah  
71 et al., 2012; Laloy et al., 2010; Vrugt et al., 2003; Wu and Liu, 2012) or crop modelling (Makowski et  
72 al. 2006 ; Varella et al., 2010b). In these approaches, the parameters are considered as stochastic  
73 variables defined by the prior distribution of probability. The process aims to sample the posterior  
74 distribution of the parameters leading to the statistically most relevant simulations.

75 Traditionally, it has been difficult to estimate the posterior distribution of parameter estimates  
76 and/or the model output predictions, but the use of Markov Chain Monte Carlo (MCMC) simulations  
77 (Metropolis et al., 1953; Vrugt et al., 2009b) has made this task easier. The basis of these methods is a  
78 Markov chain, which generates a random walk through the search space and iteratively visits solutions  
79 with stable frequencies. To do this, an MCMC algorithm generates trial moves from a current position  
80 in the parameter space, defined by the actual position in the Markov chain, to a new position in the

81 parameter space. The earliest and most widely used MCMC approach is the Random Walk Metropolis  
82 (RWM) algorithm (Metropolis et al., 1953). One of the particularities of the algorithm lies in the use  
83 of the Metropolis acceptance probability ratio (Metropolis et al., 1953) as a selection rule to decide  
84 whether or not the candidate parameter set could replace its parents. The result of the algorithm is a  
85 Markov chain that, for the values that are sufficiently far from the starting point, has a unique  
86 stationary distribution with stable frequencies stemming from the underlying probability density  
87 function (pdf).

88 In 1970, Hastings extended the original MCMC to include non-symmetrical proposal  
89 distribution. Called the Metropolis Hastings (MH) algorithm, this extension became the basic building  
90 block of many existing MCMC sampling schemes. In the 1990s, much research was devoted to  
91 Markov chain sampling (e.g., Gilks et al. 1996; Gelman et al., 1997; Brooks, 1998). Although this  
92 research improved the efficiency of MCMC algorithms, they remained inefficient when confronted  
93 with posteriors with very heavy tails and with posterior model output prediction surfaces that  
94 contained multiple local optima. Recognizing the limitations of previous MCMC schemes, ter Braak  
95 (2006) developed the Differential Evolution-Markov Chain (DE-MC) method, which can run  
96 simultaneously and in parallel with several Markov chains and uses a genetic algorithm for estimating  
97 parameter evolution. DE-MC solves the RWM practical problem of choosing an appropriate scale and  
98 orientation for the jumping distribution. Vrugt et al. (2008a, 2009a) proposed a new MCMC sampler  
99 called the Differential Evolution Adaptive Metropolis (DREAM) algorithm. DREAM is a follow-up of  
100 the DE-MC method and an adaptation of the Shuffled Complex Evolution Metropolis (SCEM-UA)  
101 global optimization algorithm (Vrugt et al., 2003). The authors showed how using self-adaptive  
102 randomised subspace sampling, with explicit consideration of aberrant trajectories, could still enhance,  
103 sometimes considerably, the efficiency of the DE-MC algorithm. Vrugt et al. (2009a) demonstrated  
104 that there was an optimal choice for the multiple of the difference of two randomly chosen members  
105 from remaining chains used in the genetic algorithm. The advantages of DREAM are summarised  
106 here. First, DREAM solves two important problems. One is the automatic selection of an appropriate  
107 scale and orientation of the proposal distribution during evolution towards the posterior distribution  
108 (i.e., self-adaptive randomized subspace sampling). The second one is the efficient accommodation of

109 heavy-tailed and multimodal target. Unlike the SCEM-UA algorithm, DREAM can maintain a detailed  
110 balance and ergodicity while showing good efficiency for complex and highly non-linear and  
111 multimodal target distributions (Vrugt et al., 2009a). DREAM also solves limitations such as the need  
112 to choose the starting values and the unlimited number of parameters that could be optimized at the  
113 same time (Makowski et al., 2002). Finally, and most recently, Vrugt et al. (2011) have shown how  
114 DREAM could be enhanced using parameter sampling from past states of the genetic evolutionary  
115 chains, leading to the DREAM-ZS algorithms (Vrugt et al., 2011; Laloy et al., 2012). Let's also  
116 mention that in the recent years, another suitable solutions emerged which consist to consider  
117 simultaneously parameter optimization and data assimilation (Vrugt et al., 2006, Mansouri et al.,  
118 2013).

119 In recent years, the debate has focused on the use of a formal or informal approach for  
120 specifying the likelihood function (Beven et al., 2008; Schoups and Vrugt, 2010; Vrugt et al. 2008b,  
121 2009b). Informal likelihood functions have been proposed as a pragmatic approach to uncertainty  
122 estimation in the presence of complex residual error structures. Importance sampling algorithms, such  
123 as the Generalised Likelihood Uncertainty Estimation (GLUE) method (Beven and Binley, 1992), are  
124 becoming very popular because they have the potential to deal with estimation uncertainty problems  
125 where simple theoretical likelihood assumptions are not appropriate (Beven and Binley, 1992; Beven,  
126 2008; Vrugt et al., 2009b). For example, Varella et al. (20010b, 2011) investigated characterizing soil  
127 properties in agricultural fields by inverting the STICS dynamic crop model, using the observations  
128 conducted in those fields by remote sensing or yield monitoring. This method, however, involves  
129 discretising the parameter space in order to perform optimization, and such an approach could lead  
130 to an inaccurate representation of the posterior parameter distribution when the model parameters are  
131 numerous (Makowski et al., 2002).

132 Alternatively, the formal approach starts from an assumed statistical model for the residual  
133 errors (Joseph and Guillaume, 2013 ; Laloy et al., 2010 ; Vrugt et al., 2009b). This model, which is  
134 specified *a priori*, is then used to derive the appropriate form for the likelihood function that links the  
135 model output with the real-life measurements and that should therefore correctly sample the high-  
136 probability density region of the parameter space. MCMC simulations then allow behavioural

137 solutions to be separated from non-behavioural ones, using a threshold based on the sampled  
138 probability mass. Typically, the residual error assumptions can be classified into three groups relating  
139 to (i) error variance, (ii) error distribution and (iii) error correlation. The advantage of the formal  
140 approach is that error model hypotheses are stated explicitly and their validity can be verified *a*  
141 *posteriori* (e.g., Schoups and Vrugt, 2010). The formal approach, however, has been criticised for  
142 relying too heavily on residual error assumptions that do not reflect reality in many applications  
143 (Beven et al., 2008). For example, considering that the errors are independent and identically  
144 distributed, following a normal distribution with zero mean and constant variance  $\sigma^2$ , the statistical  
145 error model would result in the standard least squares (SLS) approach (Box and Tiao, 1973). In many  
146 cases, however, and especially in agricultural research, the errors are correlated, non-stationary and  
147 non-Gaussian. Correlations between model residuals often arise when several measurements are  
148 performed at different dates in a given site-year. Site-year characteristics have a strong influence on  
149 observations and, as only a part of the between site-year variability can be predicted by crop models,  
150 model residuals obtained in a given site-year have different variances and are often correlated  
151 (Wallach et al., 2006).

152         The main objective of this paper is to extend the available parameter estimation tools of the  
153 STICS soil-crop model. Currently, DREAM and DREAM-ZS are probably among the most optimized  
154 MCMC algorithms than can offer genericity and robustness in the parameter sampling process. On the  
155 other hand, the STICS model is widely used and its ability to simulate contrasted situations and to  
156 adapt to new species is well recognised; to date, however, parameter optimization is rarely obtained  
157 using MH algorithms. The first aim of this paper is therefore to extend the parameter estimation  
158 techniques available for the STICS model by using the DREAM-ZS scheme and to assess the coupling  
159 of both algorithms.

160         At another level, in-field measurement errors associated with crop modelling experiments is  
161 not a trivial problem. To improve the computational efficiency of the sampling MCMC algorithms, the  
162 expert knowledge could be expressed at the process initialisation stage through a more appropriate  
163 definition (e.g., tightening) of the parameters' *prior* distribution. In our opinion, however, it should  
164 also advantageously appear in the likelihood function, making it possible to take account of systematic

165 error measurements. In this context, and using a formal representation of error assumptions, a new  
166 version of the likelihood function was derived that makes explicit use of the coefficient of variation  
167 (CV) of the measurements and which should be able to account for heteroscedastic error cases.

## 168 2. Material and methods

### 169 2.1. Case study

170 The data used in this paper derive from an experiment designed to study wheat growth  
171 response (*Triticum aestivum* L., cultivar Julius) under different nitrogen fertilization levels. The  
172 experimental blocks were prepared on two soil types (loamy and sandy loam), corresponding to the  
173 agro-environmental conditions of the Hesbaye region in Belgium. The measurements were the results  
174 of four repetitions by date, nitrogen level, soil type and crop season. Each repetition was performed on  
175 a small block (2 m × 6 m) within the original experiment as a complete randomised block distribution,  
176 spread over the field within each soil type, to ensure measurement independence. A wireless  
177 microsensor network was used to continuously characterize the soil (water content, suction,  
178 temperature at two depths: 30 and 50 cm) and the atmosphere (radiation, temperature, relative  
179 humidity) within the vegetation. Pluviometry data were also acquired in the experimental field.  
180 Biomass and soil nitrogen content were regularly measured manually.

181 This paper focuses on the biomass growth, described by the MASEC output within the STICS  
182 model, over three years (crop seasons 2008-09 to 2010-11). Two fertilization levels were considered in  
183 this study: crop growth (i) without nitrogen feeding and (ii) under a nitrogen level of 180 kgN.ha<sup>-1</sup>  
184 applied in three fractions and according to three equivalent doses, respectively at the tillering (Zadoks  
185 stage 23), redress (Zadoks stage 30), and last-leaf stages (Zadoks stage 39). The above ground biomass  
186 measurements were performed at a bi-weekly interval from mid-February (about Julian day 410) until  
187 harvest. The above ground biomass was defined here as the sum of straw and grain yields. The  
188 measurements were performed on dried samples, corresponding to the sampling of three adjacent  
189 50cm rows.

190 Table 1 summarizes the different identified cultural situations (CS) according to the cropping  
191 seasons and the stresses events. For each of the two crop cycles of the first season (CS 1 and 2), ten  
192 measurements were performed. Nine aboveground biomass measurements were made for each  
193 nitrogen level of the season 2009-10 (CS 3 and 4) while five biomass samples were taken during the  
194 last season (CS 5 and 6).



195 **Table 1: The different cultural situations (CS) and the stress effects**

Stress effect	No nitrogen stress 180kgN.ha <sup>-1</sup>	Nitrogen stress 0kgN.ha <sup>-1</sup>
No water stress Season 2008-09	CS 1 Calibration dataset	CS 2 Calibration dataset
Water stress #1 Season 2009-10	CS 3 Calibration dataset	CS 4 Calibration dataset
Water stress #2 Season 2010-11	CS 5 Validation dataset	CS 6 Validation dataset

196

197 **2.1.1. Calibration dataset**

198 The first two years of experiments were used to calibrate the model. The 2008-2009 crop was  
 199 sown in late October (Julian day 297) and harvested in mid-August (Julian day 593). The yields were  
 200 quite high and close to the optimum of the cultivar, mainly because of the good weather conditions and  
 201 the sufficient nitrogen nutrition level. In the 2009-2010 season, the crop was sown in early November  
 202 (Julian day 323) and harvested a bit later than in first year (Julian day 598), due to the poor aestival  
 203 conditions. This season was characterised by significant water stress that occurred at the early season  
 204 (February) and in the early summer (July).

205 **2.1.2. Validation dataset**

206 The last year of experiments was used to perform the model validation. During the season  
 207 2010-11, the measured yields were close to the ones observed in 2009-10. However, a lower number  
 208 of tillers and fewer grains per ear were observed. This was a consequence of strong climate-induced  
 209 stresses, namely an important water deficit and high temperatures at spring (from the middle of March  
 210 till the end of May). Owing to the return of rain at early summer, the grains have been correctly filled  
 211 but the straw yield has remained really poor.

212

213 **2.2. Model description**214 **2.2.1. The STICS crop model**

215 The STICS crop growth model (INRA, France) used in this study has been described in  
 216 several papers (Brisson et al., 1998; Brisson et al., 2003; Brisson et al., 2009). STICS is a generic soil-  
 217 crop model that can simulate a broad range of crops. It simulates the water, carbon and N dynamics in  
 218 the soil-plant-atmosphere system on a day-by-day basis. It allows to take into account the effect of

219 water and nutrient stress on development rate (Palosuo et al., 2011). It requires daily weather data  
220 inputs (i.e., minimum and maximum temperatures, total radiation and total rainfall, vapour pressure  
221 and wind speed).

222         Within STICS, the eco-physiology of aboveground growth is driven by a classic carbon  
223 balance : the leaf development allows the interception of the solar radiation, which is converted into  
224 biomass and later oriented towards harvestable organs. The whole plant phenology of aboveground  
225 growth is driven by the degree-day thermal index [ $^{\circ}\text{C}\cdot\text{day}$ ].

226

### 227         **2.2.2. Parameter assumptions**

228         Nine parameters involved in the aboveground biomass growth simulation were selected to be  
229 optimised. However, in order to avoid over-parameterization (Varella, 2011; Varella et al., 2010b), the  
230 selected parameters were chosen as not being all directly linked to the formalism of the simulated  
231 variable (MASEC) : we considered parameters involved in the phenology (*stlevamf*, *stamflax*), the leaf  
232 area development (*dlaimaxbrut*, *durvieF*), parameters directly related to biomass growth (*efcroijuv*,  
233 *efcroirepro*, *efcroiveg*) and finally related to water and nitrogen stresses (*psisto*, *INNmin*). The  
234 remaining parameters of the species were fixed at the suggested default values (Brisson et al., 1998;  
235 2003).

236         Table 2 summarizes the studied parameters, their initial value and their prior distribution. In  
237 this table, the ILEV, IAMF and ILAX stages correspond respectively to the stage of emergence, the  
238 day when the leaf growth rate is maximal (AMF stage), and the day when the maximal leaf area index  
239 (LAI) is reached. The complete senescence of the crop, conducted by the *durvieF* parameter is reached  
240 a few days before maturity of the crop. The radiation use efficiency is known to be different during  
241 plant growth. It is lower during the juvenile phase, which extends between emergence (ILEV) and  
242 AMF stage (IAMF). It is higher during the vegetative stage, which occurs between AMF stage and  
243 flowering, and during the reproductive phase. As an illustration, the Figure 1 shows the biomass  
244 measurements performed during the crop season 2008-2009 with the corresponding standard  
245 deviation.

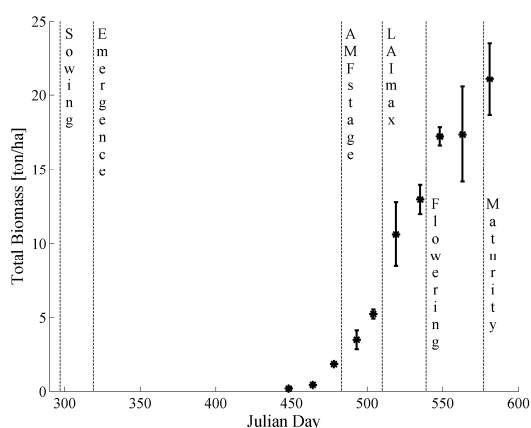
246 **Table 2 : Initial parameters values and prior distribution**

Parameter	$\theta^{init}$	Prior values	Unit	Definition
<i>dlaimaxbrut</i>	4.5E-4	[0 - 4E-3]	$m^2_{leaf} \cdot (plant)^{-1} \cdot (^\circ C \cdot day)^{-1}$	Maximum rate of LAI daily increase
<i>stlevamf</i>	255	[0 - 400]	$^\circ C \cdot day$	Duration between ILEV and IAMF stages
<i>stamflax</i>	350	[0 - 500]	$^\circ C \cdot day$	Duration between IAMF and ILAX stages
<i>durvieF</i>	220	[0 - 500]	$^\circ C \cdot day$	Maximal lifespan of an adult leaf
<i>efcroijuv</i>	1.8	[0 - 4.5]	$g \cdot MJ^{-1}$	Radiation use efficiency during juvenile phase
<i>efcroiveg</i>	4.25	[0 - 10]	$g \cdot MJ^{-1}$	Radiation use efficiency during vegetative stage
<i>efcroirepro</i>	4.25	[0 - 9]	$g \cdot MJ^{-1}$	Radiation use efficiency during grain filling phase
<i>INNmin</i>	0.360	[0 - 1]	/	Minimum value of Nitrogen Nutrition Index allowed
<i>psisto</i>	15	[1 - 20]	bar	Absolute value of the potential of stomatal closing

247

248 The lower and upper boundaries of the *prior* parameter distribution were slightly modified  
 249 compared with the original OptimisTICS package. They were reduced in order to ensure faster  
 250 convergence, but they were kept wide enough to produce a sufficiently high parameter space.

251



252

253 **Figure 1: Biomass measurements (mean values and standard deviations),**  
 254 **and principal phenological stages of the crop during the cultural season 2008-09.**

255

256 The parameters were sampled/optimized on the first four contrasted cultural situations, *i.e.*  
 257 corresponding to the climatic input data of season S.2008-09 and S.2009-10, and to the nitrogen level  
 258 0 and 180kgN.ha<sup>-1</sup> (CS 1-4 in table 1). A total of 38 biomass measurements were used to identify the  
 259 nine parameters. Once the parameters sampled, the model was then evaluated on the crop season  
 260 2010-11 (CS 5 and 6).

261

## 262 2.3. Bayesian theorem, error assumptions and adapted likelihood function

### 263 2.3.1. The Bayes theorem

264 According to the Bayes theorem, the posterior probability density function (pdf)  $\pi(\theta|Y)$  is  
 265 given by following equation:

$$266 \quad \pi(\theta|Y) = \frac{\pi(Y|\theta)\pi(\theta)}{\pi(Y)} \quad (1)$$

267 In this expression,  $\theta$  and  $Y$  represent the vectors of the parameters and the measurements, respectively,  
 268 and  $\pi(\theta|Y)$  represents the pdf of the parameters given the observed data and/or measurements. This  
 269 probability constitutes the *posterior probability* of the estimated parameters.  $\pi(\theta)$  is the probability  
 270 distribution of the parameters to be estimated. This constitutes the *prior probability*, referring to the  
 271 *prior* knowledge existing about the parameters. It usually consists of a uniform distribution limited by  
 272 realistic lower and upper bound parameter values.  $\pi(Y)$  is the probability distribution of the observed  
 273 data. It is a constant determined by the requirement that the integral of the posterior distribution  $\pi(\theta|Y)$   
 274 over the parameter space must equal 1.  $\pi(Y|\theta)$  is the probability distribution of the measurements given  
 275 the parameters and is referred to as the *likelihood function*. Its value is determined from the probability  
 276 distribution of the error  $\varepsilon_i$  between modelled and observed data :

$$277 \quad \varepsilon_i(\theta|Y, X) = \hat{y}_i(X, \theta) - y_i, \quad i = 1, \dots, n \quad (2)$$

278 where  $n$  is the total number of observations,  $\hat{y}_i(\theta, X)$  is the  $i^{\text{th}}$  modelled value, according to model inputs  
 279  $X$  and model parameters  $\theta$  and  $y_i$  is the corresponding observation.

280 The problem lies in estimating the likelihood function. Assuming that errors, also called  
 281 residuals (Equation 2), are uncorrelated and Gaussian-distributed (Equation 3),

$$282 \quad \varepsilon_i \approx N(0, \sigma_i^2) \quad (3)$$

283 the likelihood function can be simplified, taking the following form (Equation 4; Box and Tiao, 1973):

$$284 \quad \pi(Y|\theta) = \prod_{i=1}^n \frac{1}{\sqrt{2\pi\sigma_i^2}} \exp\left\{-\frac{[\hat{y}_i(\theta, X) - y_i]^2}{2\sigma_i^2}\right\} \quad (4)$$

285 where  $\sigma_i^2$  is the error variance on measurement  $i$ .

286 Finally, for reasons of algebraic simplicity, numerical stability and algorithm implementation,  
 287 Vrugt et al. (2009b) proposed using the logarithm transformation of the likelihood function:

$$\pi_{\log}(Y|\theta) = -\frac{n}{2} \ln(2\pi) - \sum_{i=1}^n \ln(\sigma_i) - \frac{1}{2} \sum_{i=1}^n \left( \frac{\hat{y}_i(\theta, X) - y_i}{\sigma_i} \right)^2 \quad (5)$$

288  
 289 The actual form of Equation 5 is known as the weighted least square (WLS) function. Instead  
 290 of the  $\sigma_i^2$  value, a constant value for the error variance  $\sigma^2$  could be hypothesised. Such an assumption  
 291 would consist to consider a constant error variance whatever the measurement dates and their absolute  
 292 values. In that way, it allows simplifications to be made in Equation 5, which results in the standard  
 293 least square (SLS) form of the equation. These error assumptions (SLS and WLS), however, are both  
 294 quite strong and can be unrealistic in crop modelling (e.g., when the measurements are performed at a  
 295 same location throughout the season).

296

### 297 **2.3.2. Experimental design and residual assumptions**

298 As noted above, the SLS and WLS approaches made the assumption that the errors were  
 299 uncorrelated and (identically or proportionally) Gaussian-distributed. The experimental design was  
 300 adapted to meet part of this assumption and the original experiment was implemented as a *complete*  
 301 *randomised block distribution*.

302 Applying Fisher's three principles (Preece, 1990) – *replication*, *randomization* and *local*  
 303 *control* – allows the error variances to be estimated while increasing the precision of the experiment  
 304 (diminution of error). More precisely, *randomisation* allows an unbiased estimation of the residual  
 305 variance to be obtained, whereas *local control* (sometimes called *blocking*) increases the precision of  
 306 the experiment. The main objectives of the *complete randomised block distribution*, especially its  
 307 *randomisation* component, is to create experimental units that are as similar as possible in order to  
 308 reduce, within the blocks, the heterogeneity of the experimental conditions. This allows the spatial  
 309 correlation to be reduced and, at a lower measure, the temporal correlation between the measurements,  
 310 which then correspond to an average over replicates.

311 Each of the  $y_i$ -values and the corresponding standard  $\sigma_i$ , deviations needed for the likelihood  
 312 function calculation therefore resulted from four replicates randomly spread over the experimental  
 313 field.

314

### 315 2.3.3. Non-stationary and correlation error assumptions

316 From these in-field observations, it appeared that the averages and the standard deviations of  
 317 the total biomass measurements increased throughout the seasons, transducing a non-stationarity of the  
 318 residuals. As the first part of the results section shows, however, the CVs, expressed as the ratio  
 319 between the standard deviation and the measure (Equation 6), exhibited stationary values:

$$320 \quad CV = \frac{\sigma_i}{y_i} \quad (6)$$

321 We therefore decided to introduce CV explicitly into Equation 4 and, after log-transformation,  
 322 a revised likelihood function was obtained (Equation 7), referred here-after as CV likelihood function:

$$323 \quad \pi_{\log}(Y|\theta) = -\frac{n}{2} \cdot \ln(2\pi \cdot CV^2) - \sum_{i=1}^n \ln(y_i) - \frac{1}{2} \sum_{i=1}^n \left( \frac{\left( \frac{\hat{y}_i(\theta, X)}{y_i} - 1 \right)}{CV} \right)^2 \quad (7)$$

324 Typically, crop growth is known to be a heteroscedastic phenomenon. In that way, if the CV is  
 325 stationary over the seasons and over the years, the proposed formula will offer important advantages.  
 326 On one hand, if too few measurements are available for practical reasons (such as financial constraints  
 327 or storm events), the use of the proposed likelihood function would allow the computation of a CV  
 328 relevant for the whole crop growth cycle, which will increase the efficiency of the parameters  
 329 sampling process.

330 On another hand, ideally, the CV value should correspond exclusively to the expression of the  
 331 crop natural genetic variability. However, for practical reasons, it involves measurement errors, *i.a.*  
 332 linked to inadequate measurements sampling process or non-adapted equipment. Such errors will be  
 333 added to the natural variability and may conduct to overestimated CV values. Next to the *prior*  
 334 definition, the definition of a realistic CV value will thus also allow to express the expert's knowledge  
 335 at each step of the parameter sampling process.

## 336 2.4. Parameter identification and model output uncertainty

### 337 2.4.1. The OptimISTICS parameter optimisation package

338 The OptimISTICS package was used as a reference in this study to assess the performance of

339 the DREAM algorithm. A brief description of OptimISTICS is given here beneath, a full description  
340 can be found in Wallach et al. (2011). OptimISTICS calculates the parameter values that optimize the  
341 goodness-of-fit criterion (for example that minimize a sum of squared errors). OptimISTICS uses the  
342 Nelder-Mead simplex algorithm which can be used for multidimensional minimization for any  
343 function. The simplex algorithm used is the Matlab function "*fminsearchbnd*".

344 However, crop models are complex functions of the parameters and there is no assurance that  
345 local optimization techniques will converge to the global optimum. To overcome this problem, in  
346 OptimISTICS, the simplex algorithm is run with several different starting points. The more numerous  
347 starting points used, the less the risk of missing the global optimum.

348 It is worth mentioning that the OptimISTICS package proposes different options. The software  
349 can treat the case where some parameters are genotype specific while others are common to all  
350 genotypes. It can also automatically do several sequential stages of parameter estimation. Finally, the  
351 software offers the possibility to consider different model errors, including the WLS case (Wallach et  
352 al., 2011).

353

#### 354 **2.4.2. The DREAM algorithm and the associated parameter uncertainty**

355 The origins and developments that led to DREAM were depicted in details in the introduction  
356 section. The present section and the following are focused on the advantages offered by DREAM in  
357 terms of post-data treatment.

358 Assessing the posterior distribution of the model parameters using MCMC simulations,  
359 performed with DREAM or DREAM-ZS, led to several chains that contained all the necessary  
360 information about model parameterization.

361 The first step in obtaining parameter estimates is to select, among the chains, the parameter set  
362 that offers the optimal solution ( $\theta^{opt}$ ), *i.e.* the one that optimises the convergence criterion. However,  
363 provided convergence has achieved a stationary distribution, from a statistical/methodological point of  
364 view, the information contained in each chain has the same relevance. In a second step, the marginal  
365 posterior pdfs were thus evaluated, with the concatenated information contained in each chain (e.g.,  
366 drawing their histograms). This insight should offer primal information about the quality of sampling,

367 depending on whether the histograms exhibit a pronounced mode, are bimodal or close to the prior  
 368 distribution. An interesting discussion about such observations was reported by Laloy et al. (2010).

369 When designing decision-support tools, it seems necessary for the modeller to summarize the  
 370 marginal posterior pdf in one parameter estimate. An initial step in assessing the most probable  
 371 parameter value involves calculating the posterior means (Equation 8), the corresponding standard  
 372 deviation, and eventually the correlation coefficients between the generated parameter samples.

$$373 \quad \theta^{mean} = \frac{1}{n \times 2 \times d} \sum_{i=1}^{n \times 2 \times d} \theta_i \quad (8)$$

374 In this equation,  $d$  is the number of sampled parameters and  $2 \times d$  is the number of chains,  $n$  is the  
 375 number of last elements in a chain of the sampling process, when each chain exhibits a stable posterior  
 376 parameter distribution, and  $\theta_i$  is one of the numerous probable values for the parameters. The number  
 377 of chains was fixed as two times the number of parameters ( $2 \times d$ ). In this study, the last  $n=1000$   
 378 elements of each chain were compiled in order to calculate the mean of each parameter value.

379

### 380 **2.4.3. The DREAM algorithm and the output predictive uncertainty**

381 In addition to parameter uncertainty, we were also interested in the predictive uncertainty  
 382 linked to the corresponding model output. The posterior distribution of the model parameters derived  
 383 with DREAM or DREAM-ZS contains all the information needed to summarize predictive uncertainty  
 384 (Vrugt et al., 2009b). A common and easy approach is to evaluate the model output  $Y$  for the last  $P$   
 385 parameter sets of each chain ( $2 \times d$  chains) when convergence has been achieved for a stationary  
 386 distribution. The so-obtained model output set  $\{Y_j, j = 1, \dots, 2 \times d \times P\}$  is summarized in the desired way,  
 387 *e.g.* by computing the 2.5% and 97.5% percentiles of the model predictions, which difference  
 388 corresponds to the 95% uncertainty boundaries. This predictive distribution includes only the effect of  
 389 parameter uncertainty (Vrugt et al., 2009b). The wider the parameter posterior distribution, the wider  
 390 the 95% boundaries. In addition, the 50% percentile simulation could also be used to evaluate model  
 391 performance, and be compared with the  $f(X, \theta^{mean})$  simulations.

392 In this case, the last 1.000 sets were no longer considered. To reduce the simulation time, the  
 393 dataset was reduced to the last 30 values of each Markov chain. Since there are 18 chains



394 ( $2 \times d$  parameters), the parameter uncertainty evaluation in the model MASEC output was summarized  
395 in the percentile computation of  $30 \times 18 = 540$  simulations.

396

#### 397 **2.4.4. The sampling process**

398 Even if the STICS model has been widely used to study and simulate wheat growth, Belgian  
399 cultivars differ from French ones, notably by their phenology and yields. For a first evaluation of the  
400 model, the original parameters file of the wheat species remained at the suggested default values  
401 (Brisson et al., 1998; 2003) included in the STICS software. This case was referred to as the *initial*  
402 *case* and  $\theta_{init}$  represents this initial parameter set.

403 As a first parameter optimisation technique, the OptimISTICS package was used. In  
404 accordance with the requirements of the DREAM algorithm (see below), 18 starting points were used  
405 and randomly generated among the prior knowledge one owned about parameter, *i.e.* it's *a priori*  
406 distribution. When running OptimISTICS, the residuals were considered as being independent errors,  
407 with zero expectation and the same variance, which corresponds to the same assumptions as for the  
408 SLS case run with the DREAM algorithm (see below). This case is referred later as OptimISTICS-  
409 SLS. The selected parameter set was the one that gave the minimum error (Wallach et al., 2011), *i.e.*  
410 the one that should offer the optimal solution ( $\theta^{opt}$ ).

411 The DREAM-ZS algorithm was then used to perform parameter sampling of the STICS  
412 model. To evaluate its performance, various assumptions about the error measurements were  
413 considered and taken into account for different likelihood functions.

414 The first case made use of a classical sum of squared error to represent the likelihood function,  
415 in line with the frequentist approaches. Since simplification appeared in the algorithm, the constant  
416 standard deviation disappeared and the measurements were considered only by their mean value. This  
417 case was referred to as the DREAM-SLS case, and  $\theta_{SLS}$  represented the corresponding optimised  
418 parameter set. The second case corresponded to the weighting, within the likelihood function  
419 computation, of residual data by the nominal standard deviation calculated on the basis of the four  
420 replicates of in-field measurements, and relied on implementing Equation 5. This case, corresponding

421 to the DREAM-WLS, was represented by  $\theta_{WLS}$ . Finally, DREAM's ability to retrieve parameter values  
 422 was evaluated against the error measurement assumption making an explicit use of the CV (Equation  
 423 7). This case will be referred as DREAM-CV. Table 3 summarizes all the error measurement  
 424 assumptions.

425 With regard to the DREAM options, the toolbox was run a maximum of 22,500 times, which  
 426 corresponded to 2,500 evaluation functions multiplied by the number of parameters ( $d = 9$ ). This value  
 427 was checked on preliminary studies to ensure convergence. The number of Markov chains was fixed at  
 428 18 because there were nine parameters to be estimated ( $MC \geq 2d$ , Vrugt et al., 2009a).

429 In each cases, a single-step calibration procedure, involving all the variables (i.e. the MASEC  
 430 output of the 4 CS) and all the parameters to optimize, was used instead of a multiple-step  
 431 optimization procedure (Guillaume et al., 2011).

432

433 **Table 3: The different cases considered for measurements errors**

Case	Error assumption	Error value
OptSTICS-SLS & DREAM-SLS	Variance fixed for all measurements (whatever date or observation value)	-
DREAM-WLS	Nominal variance value computed from replications of observed values	$\sigma_i$
DREAM-CV	Global CV value computed from all replications of observed values	0.145

434

### 435 **2.5. Evaluation of the global model output estimates**

436 A crop model is a good representation of reality if it can be used to predict observable  
 437 phenomena in the range for which it was calibrated (Loague and Green., 1991). This underlines the  
 438 need to define criteria that will determine whether a model is 'acceptable', in pursuit of set objectives.  
 439 The first criterion is the Root Mean Square Error (RMSE):

$$440 \quad RMSE = \sqrt{\frac{1}{n} \sum_{i=1}^n (y_i - \hat{y}_i(X, \theta_{1,\dots,d}^{post}))^2} \quad (9)$$

441 where  $n$  is the number of observations,  $y_i$  is an available observation of the  $Y$  measurement vector, and  
 442  $\hat{y}_i$  is the corresponding simulated value, which relies on the vector  $X$  of inputs.  $\theta_{1,\dots,d}^{post}$  represents the  
 443 vector of  $d$  parameter estimated on the *posterior* distribution, using one of the proposed techniques.

444 The model efficiency (EF) criterion presents an upper boundary, which facilitates its  
 445 interpretation and makes it suitable for comparing different situations:

$$446 \quad EF = 1 - \frac{\sum_{i=1}^n (y_i - \hat{y}_i(X, \theta_{1,\dots,d}^{post}))^2}{\sum_{i=1}^n (y_i - \bar{y}_i)^2}, \quad EF \leq 1 \quad (10)$$

447 If the model is perfect, then  $y_i = \hat{y}_i$  for each  $i$ , and  $EF = 1$ .

448 Ultimately, the normalised deviation (ND) criterion shows the tendency of the model to  
 449 provide under- or over-estimations, overall, of the real case. This parameter can be positive or  
 450 negative, but is ideally equal to zero.

$$451 \quad ND = \frac{\sum_{i=1}^n \hat{y}_i(X, \theta_{1,\dots,d}^{post}) - \sum_{i=1}^n y_i}{\sum_{i=1}^n y_i} \quad (11)$$

452 RMSE, EF and ND are rarely used alone for evaluating model quality. Brisson et al. (2002)  
 453 and Beaudoin et al. (2008) used RMSE, EF and ND jointly, on the basis that model calibration or  
 454 validation is accurate if the *RMSE* is relatively low compared with the mean of the observations, and if

$$455 \quad \begin{aligned} EF &\geq 0,5 \\ |ND| &\leq 0,1 \end{aligned} \quad (13)$$

456

## 457 **2.6. Software availability**

458 The software programs (STICS-OptimiSTICS and DREAM) are libraries of Matlab<sup>®</sup> functions  
 459 divided into several sub-packages. The STICS interface sub-package is based on the OptimiSTICS  
 460 codes and is responsible for managing the STICS simulations and their inputs and outputs. The  
 461 OptimiSTICS codes were obtained upon request by the authors ([emmah\\_web@paca.inra.fr](mailto:emmah_web@paca.inra.fr)). This  
 462 sub-package writes inputs and parameter values into the ASCII files read by STICS, called the STICS  
 463 executable function, and reads the model outputs from the ASCII files written by STICS.

464 The DREAM and DREAM-ZS source codes were obtained from the developer  
 465 ([jasper@uci.edu](mailto:jasper@uci.edu)). Interested users should contact him directly. Other options specific to the DREAM

466 toolbox were discussed by Vrugt et al. (2008a, 2009a).

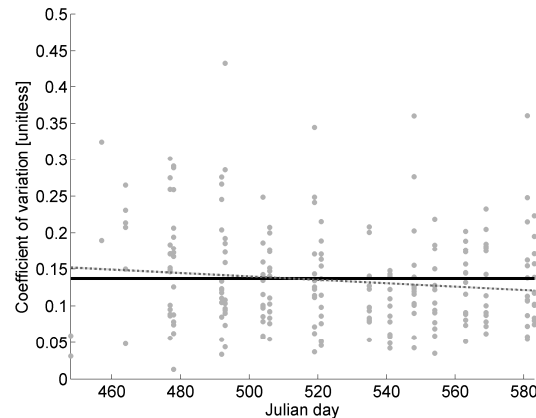
### 467 3. Results and discussions

#### 468 3.1. Spatial and temporal independence of the biomass coefficients of variation

469 First, the value of each individual  $CV$  was calculated for the data obtained for each soil type  
 470 (2), nitrogen level (7) and date of measurement ( $\pm 10$  per season) (Figure 2) in the original experiment.  
 471 The linear regression applied to the whole data set took the following form:

$$472 \quad CV = a \cdot Day + b \quad (14)$$

473 with 'Day' being the Julian day of the measurement, and  $a$  and  $b$  the parameters. The  $a$  slope  
 474 and  $b$  parameters were respectively equal to  $-0.0002$  (with a 95% confidence interval  $[-0.0005 ;$   
 475  $+2.698 \cdot 10^{-5}]$ ) and  $0.2555$  (with a 95% confidence interval  $[0.1187 ; 0.3922]$ ). Considering that (i) the  
 476 block distribution was a complete randomized experiment, (ii) the 95% confidence interval of the  $a$   
 477 slope parameter included the zero value and (iii) that the coefficient of determination  $R^2$  was low  
 478 (0.0139), the measurements could be considered as being independent. A mean  $CV$  value was  
 479 computed from all measurements (0.145) and introduced in Equation 7.



480

481 **Figure 2: Coefficients of variation (CV) of the total biomass measurements (grey dots).**  
 482 **Overall mean value (solid black line) and linear regression (dashed grey line - Eq. 14).**

483

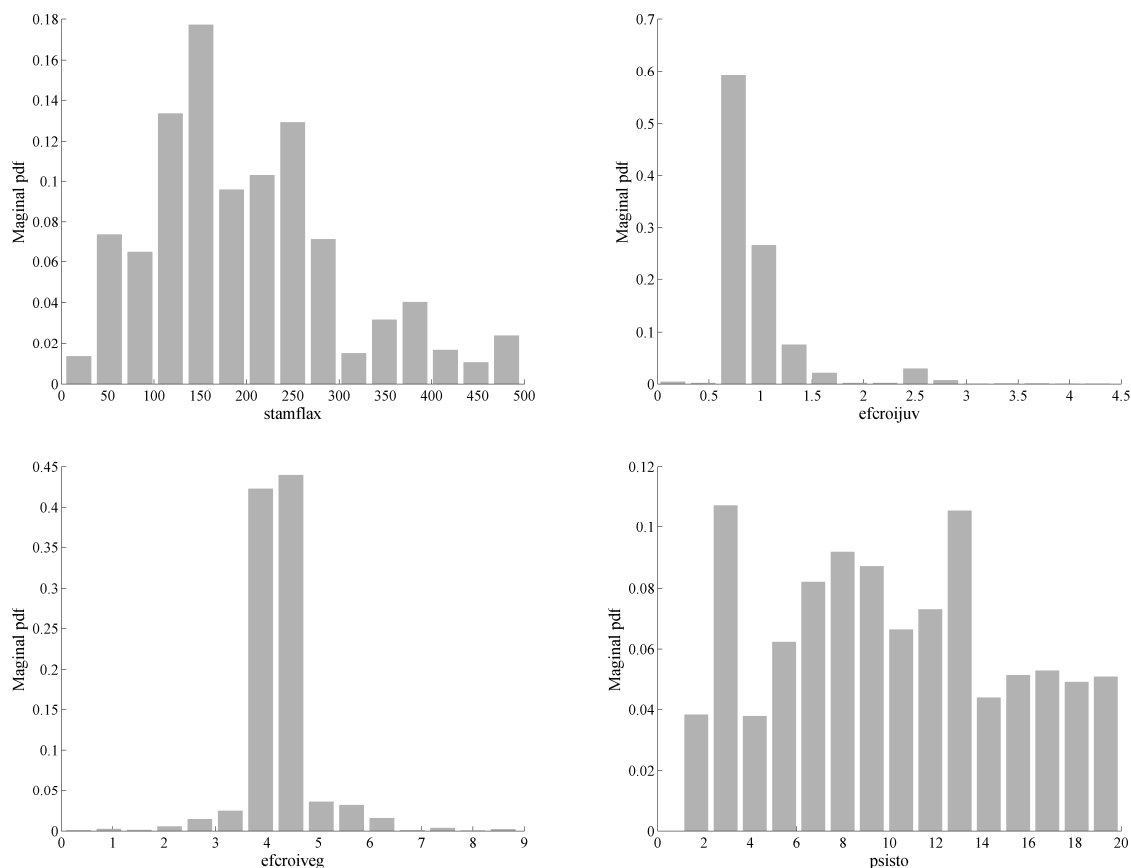
#### 484 3.2. Parameters identification

485 As an example, Figure 3 presents the marginal pdf of parameters estimates when the sampling  
 486 process had achieved a stationary distribution at the end of the WLS process. The results are given for  
 487 four parameters: *stamflax*, *efcroijuv*, *efcroiveg* and *psisto*. The grey bars represent the histograms  
 488 drawn using data computation from all the Markov chains.

489 Figure 3 shows four contrasted cases of marginal pdf. The parameters *efcroijuv*, *efcroiveg*  
490 exhibited a marked mode. The *efcroijuv* parameter showed a left dissymmetry in its pdf, which  
491 signified that very low values were rejected during the sampling process. The *stamflax* parameter had  
492 a relatively irregular shape, indicating some uncertainty about its most likely value. However, the  
493 existence of a probable dominant mode around 200 degree-day is clearly noticeable. Finally, the *psisto*  
494 parameter showed a pdf clearly close to its prior distribution. This observation may results from two  
495 different sources. On the one hand, the STICS model is known to have little sensitivity to the *psisto*  
496 parameter (Ruget et al., 2002). On the other hand, as the *psisto* parameter is the critical potential of  
497 stomatal closure, one may suppose that the number of observations performed during the water stress  
498 events was not high enough to parameterise the model. The plant water potential being seldom reached  
499 and/or observed in this rain fed experiment conducted under a temperate climate, the sampling process  
500 led to high uncertainty of the posterior distribution of the parameter.

501 Tables 4 and 5 present the parameter estimates at the end of the various sampling processes.  
502 Except for the *psisto* parameter, the optimised parameter set obtained with the OptimISTICS-SLS  
503 algorithm and the sampled parameter set obtained with the DREAM-SLS approach were very close. It  
504 would also appear that the close results obtained using OptimISTICS or the DREAM-SLS case did  
505 especially differ from the DREAM-WLS case for the *stamflax* parameter and the three radiation use  
506 efficiencies. Finally, apart from the *psisto* and *stamflax* parameters, the DREAM-CV approach tended  
507 to converge on the same parameter estimates obtained in the DREAM-WLS case.

508 With regard to Table 5 which focuses on the DREAM-WLS case, the mean estimators were  
509 evaluated in comparison with the absolute optimal estimates that might have been obtained through all  
510 the chains. Apart from the *stamflax*, *durvieF* and *psisto* parameters, the mean estimators were very  
511 close to the optimal estimates. The three previous parameters exhibit a marginal shape with high  
512 uncertainty (Figure 3). Such differences between the two values could result from an insufficient  
513 number of function evaluations, or might appear when the parameter to optimize has a shape without a  
514 pronounced mode, which often occurs when at least one of the parameter's *prior* boundaries is taken  
515 too close to the final value, when the parameter is physically bounded and exhibits a bimodal pdf  
516 (Laloy et al., 2010) or when it shows a tail in the posterior distribution (e.g., *stamflax* parameter).



517

518

519

520

521

**Figure 3: Marginal pdfs for the *stlevamf*, *efcroijuv*, *efcroiveg* and *psisto* parameters. Histogram of the parameter estimates at the end of the DREAM-WLS process.**

522

**Table 4: Parameter estimates  $\theta^{mean}$  at the end of the sampling processes.**

Case	OptStics-SLS	DREAM-SLS	DREAM-WLS	DREAM-CV
<i>dlaimaxbrut</i>	1.5E-3	1.4E-3	1.4E-3	1.5E-3
<i>stlevamf</i>	328	324	332	326
<i>stamflax</i>	386	406	198	321
<i>durvieF</i>	370	354	350	347
<i>efcroijuv</i>	0.69	0.41	0.98	1.06
<i>efcroiveg</i>	6.26	6.03	4.26	3.90
<i>efcroirepro</i>	4.49	4.64	5.75	5.86
<i>INNmin</i>	0.29	0.35	0.39	0.45
<i>psisto</i>	6.76	10.55	10.10	6.56

523

524

525 the possibility of studying parameter correlation (Table 5). Moderate to strong correlations were found

526 between model parameters, especially between the radiation use efficiency coefficient (*efcroijuv* and

527 *efcroiveg*) and the *dlaimaxbrut* parameters, which latter controls the overall leaf area index (LAI)

528 development. In particular the correlation between *efcroijuv* and *dlaimaxbrut* was the strongest, with a

529 correlation coefficient of -0.84. It highlighted the important effect of both parameters on LAI and

530 biomass output, during the early growth, *i.e.* before AMF stage. A high value of *dlaimaxbrut* would

531 lead to an important increase of leaf area, which would have to be compensated by a lower efficiency  
532 of radiation use.

533 The solar radiation use efficiency coefficients are strongly negatively correlated in pairs,  
534 *efcroijuv* vs. *efcroiveg* (-0.59) and *efcroiveg* vs. *efcroirepro* (-0.26). It clearly meant that an under- or  
535 overestimation of one parameter of the pairs was compensated during the next phenological stage to  
536 avoid the under- or overestimation of the global simulations in front of the measurements.

537 Overall, parameters were logically correlated in relation with the preceding stage or the stage  
538 during which they are the most expressed (*e.g.* *efcroijuv* during the *stlevamf* or *stamflax* stages), while  
539 poor correlations were observed for parameters referring to different formalisms/physiological aspects  
540 (*e.g.* *durvieF* and *psisto*).

541  
542 **Table 5: Summary of statistics of the marginal posterior parameter distribution in the DREAM-WLS**  
543 **case: optimal parameter set ( $\theta^{opt}$ ), posterior ( $\theta^{mean}$ ), posterior standard deviation (STD), and correlation**  
544 **coefficients over 18,000 generated samples.**

Parameter	$\theta^{opt}$	$\theta^{mean}$	STD	<i>dlaimaxb.</i>	<i>stlevamf</i>	<i>stamflax</i>	<i>durvieF</i>	<i>efcroijuv</i>	<i>efcroiveg</i>	<i>efcroirep.</i>	<i>INNmin</i>	<i>psisto</i>
<i>dlaimaxb.</i>	1.5E-3	1.4E-3	3.0E-4	1	-0.22	-0.47	-0.03	-0.84	-0.60	0.16	-0.05	-0.08
<i>stlevamf</i>	336	332	10.37		1	0.16	-0.19	0.29	0.49	-0.06	-0.25	0.06
<i>stamflax</i>	328	198	48.41			1	0.12	0.46	0.11	-0.15	-0.04	0.08
<i>durvieF</i>	280	350	33.91				1	0.04	-0.08	0.06	0.24	-0.03
<i>efcroijuv</i>	1.05	0.98	0.09					1	-0.59	0.01	-0.09	0.36
<i>efcroiveg</i>	4.05	4.26	0.21						1	-0.26	-0.46	-0.07
<i>efcroirep.</i>	6.86	5.75	0.69							1	0.15	0.11
<i>INNmin</i>	0.47	0.39	0.02								1	-0.27
<i>psisto</i>	13.2	10.10	2.45									1

545 Although the parameters were selected to avoid over-parameterization, it appeared that, at the  
546 end of the sampling process, some of them were sometimes highly correlated. Remembering that these  
547 parameters were not directly linked to the formalism driving the simulated output variable, these  
548 results highlighted that the information contained in the measurements were probably not sufficient to  
549 identify and accurately estimate all nine parameters. This could never have been shown with a classic  
550 Simplex algorithm as it doesn't provide any information on distributions or correlations of parameters.  
551

552 These observations suggest to adapt the experimental design to the modelling expectations.  
553 First of all, the selected parameters should be optimised on the output variable which they impact the  
554 most directly the process. In this case study, it would correspond to measure other model outputs (*e.g.*  
555 LAI measurements or phenological observations to sample *stlevamf*, *stamflax* and *durvieF*  
556 parameters). Another adaptation would be to increase the measurement frequency when needed, *i.a.*



557 during the phases where the growth is the fastest or focusing on identified stress events. Last proposal  
558 would be to increase the degree of variation in model driving variables, *i.e.* the weather sequences,  
559 and/or the controlling variables, like the assessed experimental nitrogen fertilisation level. These  
560 remarks corroborate the researches of Beaudoin et al. (2008) and Basso et al. (2010) who highlighted  
561 the importance of numerous measurements and long-term experiments, respectively for the parameter  
562 optimisation process and the study of crop yield answer as response to climatic variability.

563

### 564 **3.3. Uncertainty on the predictions for the calibration dataset**

565 As highlighted above, correlation may be strong between parameters. The strength of  
566 Bayesian techniques is that one can cope with such correlated parameter sets. After convergence, the  
567 posterior distribution of the model parameters derived with DREAM may be used to compute model  
568 outcomes ensembles. The predictive uncertainty can then be summarized by model outcomes  
569 averaging and confidence interval computation. However, in front of the important computational time  
570 needed by such a procedure, it may be interesting to use a unique parameter set. The next two  
571 paragraphs will thus focus on the comparison of the set of mean values of parameters and the  
572 simulations associated to the posterior distribution of the model parameters.

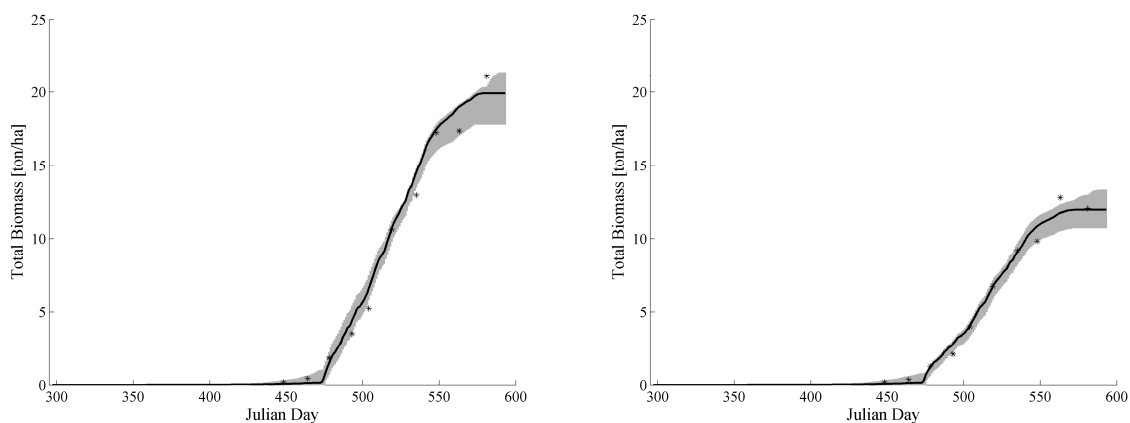
573 Figures 4, 5 and 6 present respectively the results of the model output simulations after three  
574 sampling processes: (i) the DREAM-SLS case, (ii) the DREAM-WLS case and (iii) using the realistic  
575 CV value (DREAM-CV).

576 It seems that the DREAM-SLS approach led to final selected parameter estimators that tend to  
577 bias the model output simulations (Figure 4), especially at the early stages, from sowing until Julian  
578 day 470. The same phenomenon, and pretty close simulations, were observed with the parameter set  
579 obtained at the end of the OptimiSTICS-SLS optimisation process. The corresponding growth of this  
580 physiological stage is governed mainly by the *dlaimaxbrut*, *stlevamf* and *efcroijuv* parameters. Since  
581 the *dlaimaxbrut* parameter governs the whole LAI growth, and because its value converges  
582 approximately on the same value whatever the process, this parameter could be considered as correctly  
583 estimated.

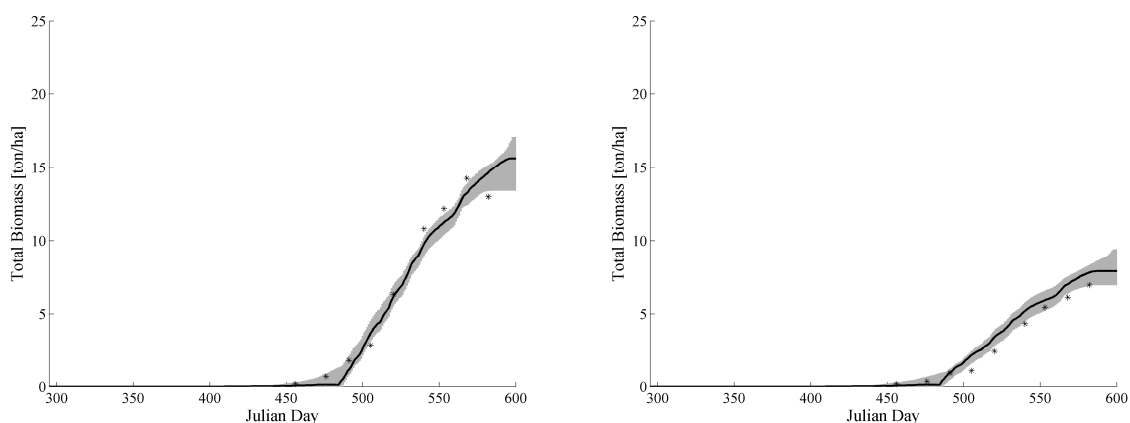
584 With regard to Tables 4 and 5, the parameter estimates obtained for *stlevamf* seemed correct

585 compared with the DREAM-WLS case, although the *efcroijuv* parameter effectively did not converge  
 586 towards realistic physical values using DREAM-SLS. The lower value during this early stage was then  
 587 compensated with a higher *efcroiveg* value applied after the *stamflax* stage, until the initiation of  
 588 flowering.

589



590



591

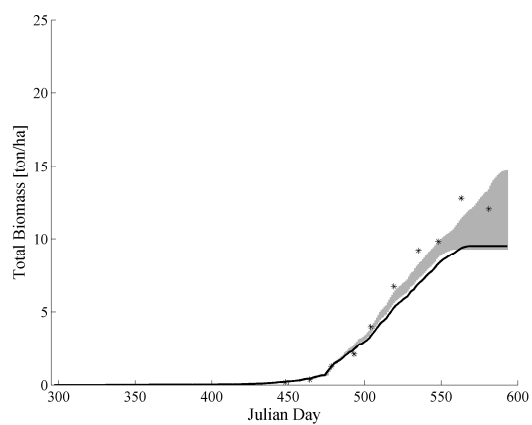
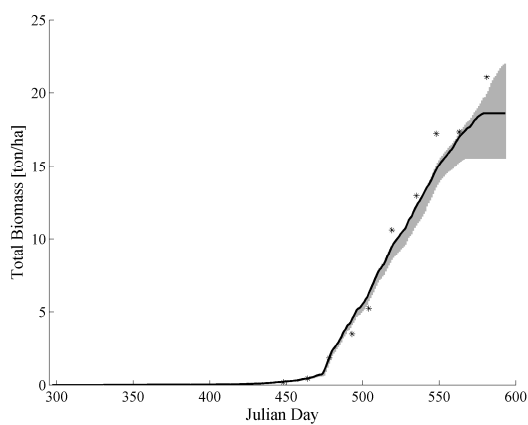
592 **Figure 4: Model output simulations for the DREAM-SLS case. No nitrogen cases (right) and 180kgN.ha<sup>-1</sup>**  
 593 **(left). Winter wheat growing season 2008-09 (upper) and 2009-10 (low). Light grey area represents the**  
 594 **95% uncertainty boundaries. Solid black line represents the simulations obtained with mean estimates for**  
 595 **parameters.**

596 In addition, when comparing the DREAM-SLS process with the DREAM-WLS approach, the  
 597 particular shape of the uncertainty boundaries is noticeable. In the DREAM-SLS case, the 95%  
 598 uncertainty boundaries exist at the start of the growth, and can be observed from Julian day 450. They  
 599 seem relatively constant throughout the growing season and for all CS. Analysing the results obtained  
 600 with the WLS likelihood function, one can immediately notice (i) the precise match of the observation  
 601 at early stage (before Julian day 500) and for the same period, and (ii) the extremely tight boundaries  
 602 around the simulated output. These observations are consistent with the assumptions made in the

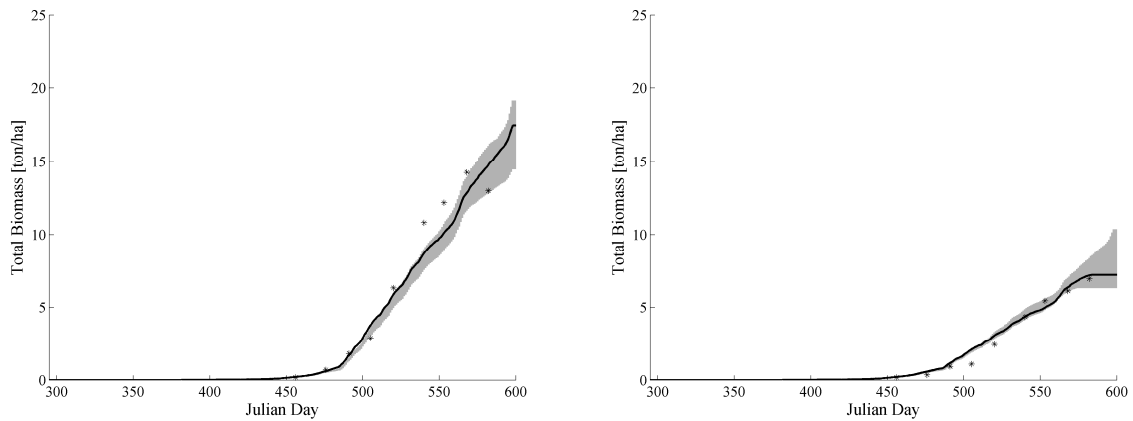
603 statistical errors model.

604 The comparison of the DREAM-WLS case (Figure 5) and the DREAM-CV approach (using a  
 605 realistic CV value of 0.145 - Figure 6) gives similar results, both in terms of uncertainty interval and  
 606 simulations based on parameter values selected with the mean estimators. In both cases, the  
 607 uncertainty intervals are very tight around the simulated output ~~small~~ at the early stages, but widen at  
 608 the end of the simulation curve. This is due to the noise/standard deviation which is increasing  
 609 proportionally to the absolute value of measurements (heteroscedasticity), as previously mentioned.  
 610 The comparison from both the DREAM-WLS and DREAM-CV cases (Figures 5 and 6) showed thus  
 611 pretty close simulations. This expected result is consistent with theory and the errors model defined  
 612 within the likelihood function, but it allowed us to conclude that the proposed formula was correctly  
 613 implemented and computationally as efficient as the WLS likelihood function. Nevertheless, since it  
 614 takes account of the natural genetic variability of crop species, the proposed formula (Equation 7)  
 615 opens the door to a new approach in parameter identification. Deeper considerations about the use of  
 616 such a function are described in the conclusion section.

617 The other observation concerns case-to-case analysis of the different cultural situations. In  
 618 general, the sampling/optimization process leads to simulations that fit the measurements properly,  
 619 taking account of nitrogen and water stresses. Since the model evaluation criteria are of poorer quality  
 620 compared with the DREAM-SLS case, it seems right that the simulation relying on the WLS or CV  
 621 likelihood function are slightly further from the measurements.

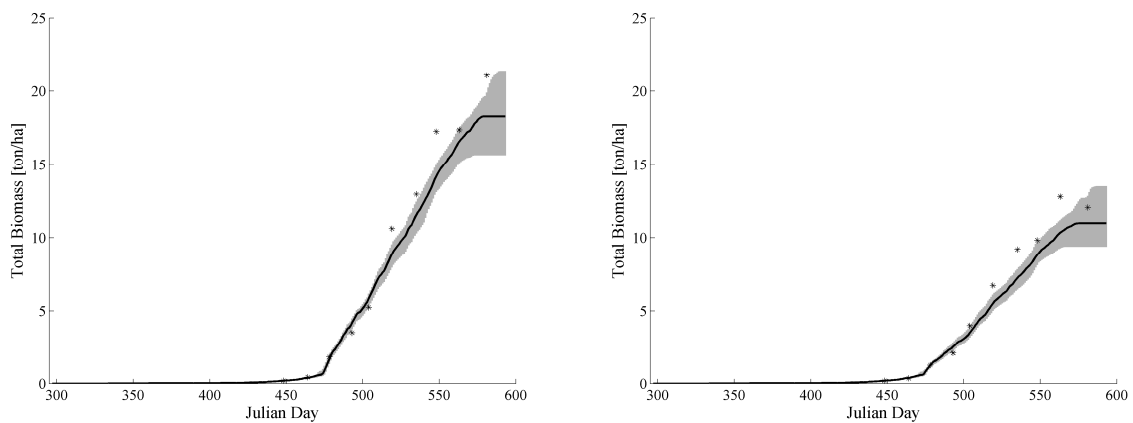


622

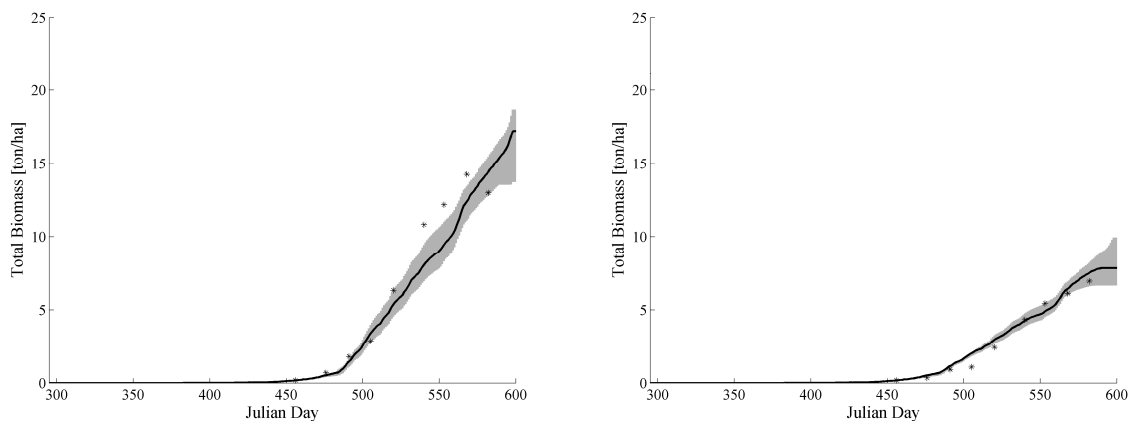


623

624 **Figure 5: Model output simulations for the DREAM-WLS case. No nitrogen cases (right) and 180kgN.ha<sup>-1</sup>**  
 625 **(left). Winter wheat growing season 2008-09 (upper) and 2009-10 (low). Light grey area represents the**  
 626 **95% uncertainty boundaries. Solid black line represents the simulations obtained with mean estimates for**  
 627 **parameters.**



628



629

630 **Figure 6: Model output simulations for the DREAM-CV (CV = 0.145) case. No nitrogen cases (right) and**  
 631 **180kgN.ha<sup>-1</sup> (left). Winter wheat growing season 2008-09 (upper) and 2009-10 (low). Light grey area**  
 632 **represents the 95% uncertainty boundaries. Solid black line represents the simulations obtained with**  
 633 **mean estimates for parameters.**

634

### 635 **3.4. Evaluation of the overall model quality**

636 Figure 7 presents the results of the model output evaluation criteria, both for the calibration

637 and validation procedures. The grey-scale histograms correspond to different model output  
638 simulations: simulations performed on the basis, respectively, of the mean parameter density estimates  
639 (light grey) and the 50% percentile of the last 540 simulations (dark grey). The horizontal black line  
640 represents the initial run of the model, based on the initial STICS parameter set.

641 In the sampling processes conducted on the calibration dataset (left graphs on Figure 7), the  
642 results of the model evaluation were greatly improved compared with the initial run. RMSE was  
643 divided at least by two. The EF criterion, already superior to 0.5, was nevertheless improved and was  
644 close to 1. The ND criterion was also enhanced, and was always lower than the expected 0.1 value.  
645 With regards to the thresholds generally considered in crop modelling (Brisson et al., 2002 ; Beaudoin  
646 et al., 2008), the model was considered has being correctly calibrated.

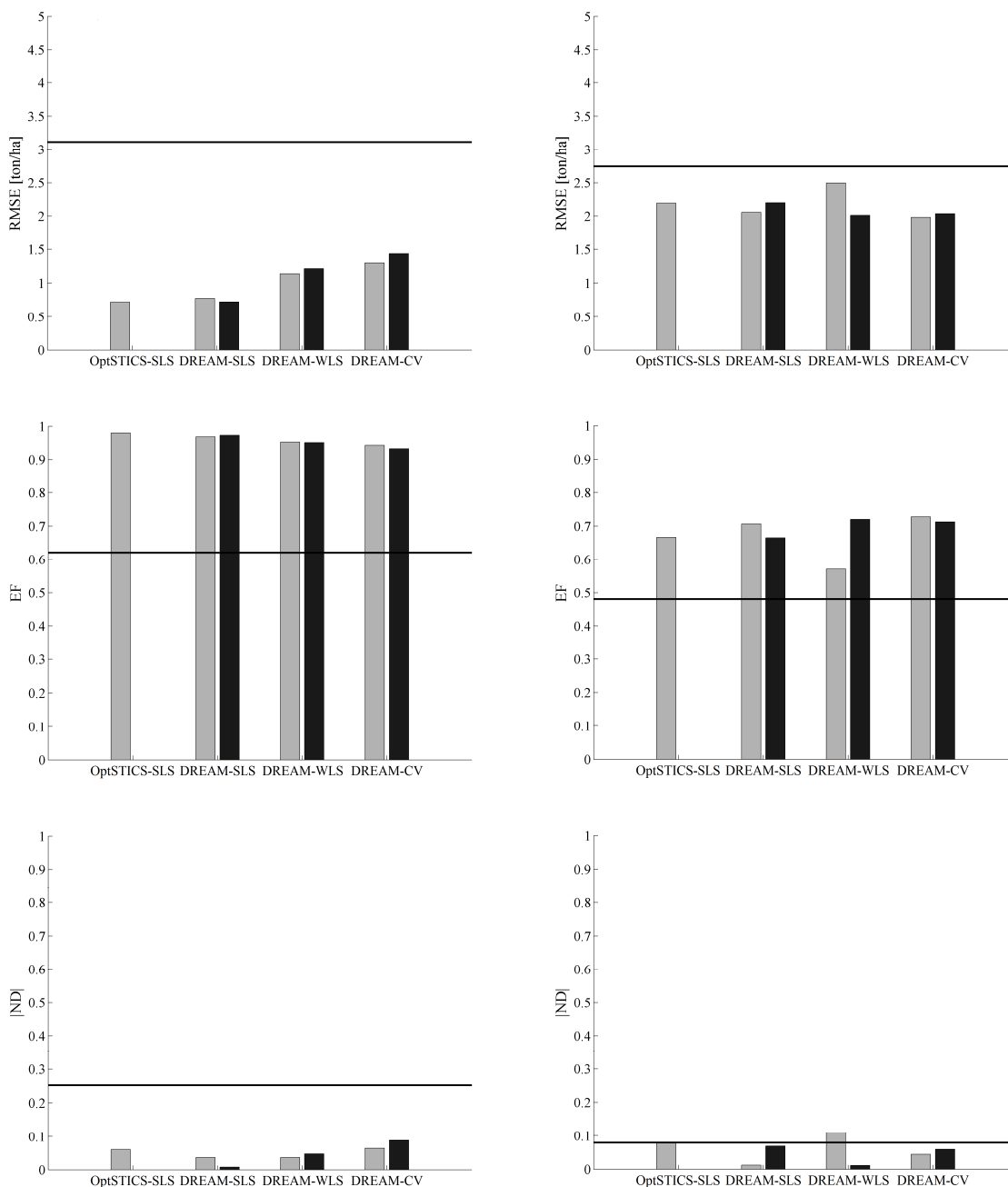
647 Comparing the various optimisation/sampling processes, it appeared that OptimiSTICS-SLS  
648 and DREAM-SLS cases always gave the better results. Their similar objective functions, i.e. the  
649 minimization of the RMSE between simulations and calibration data, explained why they converged  
650 on similar parameter set, and thus gave obviously the best RMSE on the data used for the calibration.  
651 The DREAM-WLS and DREAM-CV cases showed also and quite logically similar performances.

652 It is worth mentioning that, in all the calibration cases, the mean parameter set obtained at the  
653 end of the sampling process led to similar results than the 50% percentile computed out of the last 540  
654 simulations.

655 Considering the validation dataset (right graphs on Figure 7), the three criteria were enhanced  
656 in comparison of the initial run, even if the performances were slightly lower than in the calibration  
657 run. The RMSE was approximately 1 t/ha lower than the initial run. The model efficiency (EF) which  
658 was below the 0.5 threshold under the initial parameter set, was improved till more or less 0.65. The  
659 ND criterion, was improved under all the considered error assumptions and remained always under the  
660 validation threshold of 0.1. In presence of these results, the model was considered as validated  
661 whatever the error assumption made.

662 Concerning the intercomparison on the validation dataset, the four error assumptions led to  
663 quite similar results. One could however notice the lower quality of the simulations obtained with the  
664 mean parameter set computed at the end of the DREAM-WLS sampling process. It was shown that the

665 posterior distribution of parameters could have multimodal or dissymmetrical distributions. While the  
 666 correlation between parameters was obviously maintained during the sampling process, due to the  
 667 shape of posterior distribution, a set of parameters calculated as the mean of the last given element of  
 668 all chains may thus not necessarily represent a combination that will provide a good model evaluation,  
 669 especially when assessed on an independent/validation data set.  
 670



671

672

673

674

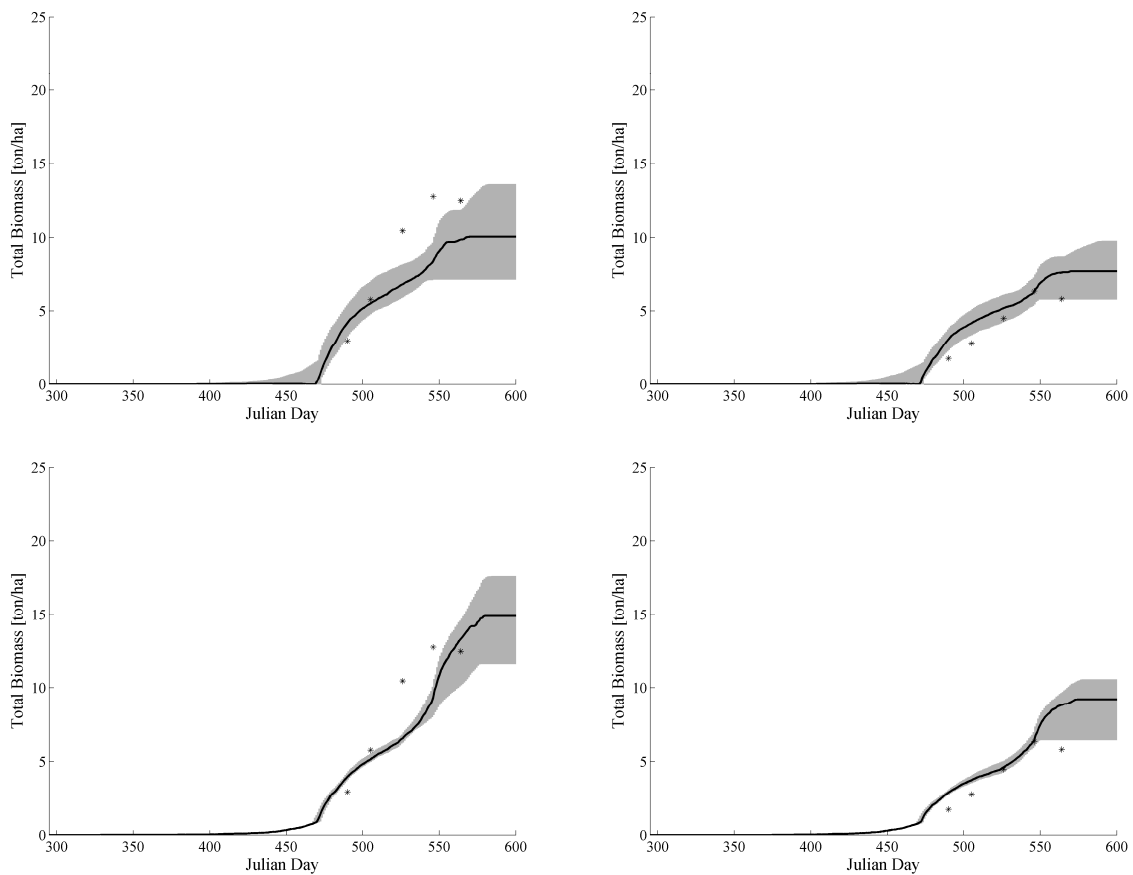
675

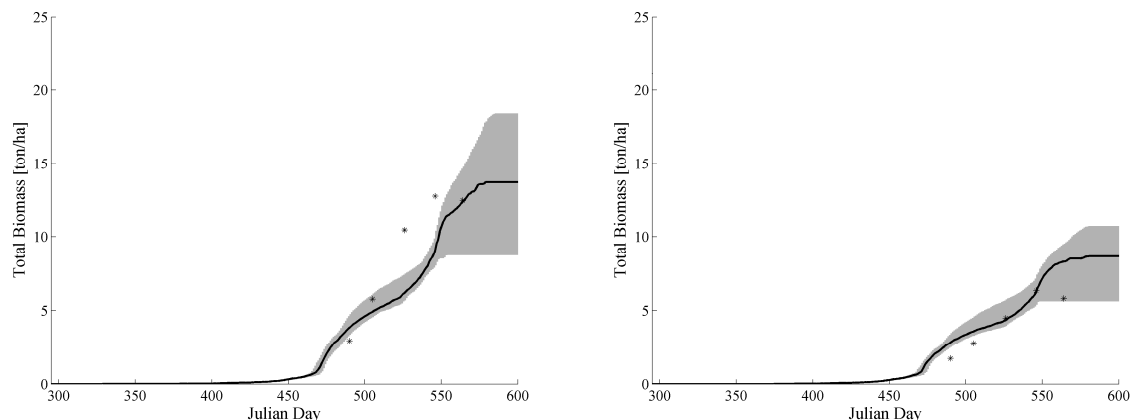
676

**Figure 7 : Model evaluation criteria based on the calibration dataset (left) and the validation dataset (right). Initial model run (horizontal black line). Model evaluation using the parameters estimated with mean density (light grey), and the percentile 50% of the 540 model output simulations (black).**

677 **3.5. Uncertainty on the predictions for the validation dataset**

678 To validate previous statements, the temporal evolution of the model's outputs were computed  
 679 for the validation dataset and for the different error assumptions (Figure 8). As previously observed, in  
 680 the DREAM-SLS case (and this was also true with the parameter set obtained with  
 681 OptimiSTICS-SLS), the simulations did not respect the biophysical behaviour of plants at early stages,  
 682 compensating later the biomass growth with higher radiation use efficiencies. The results obtained  
 683 under the 'no nitrogen' case and for the DREAM-WLS and DREAM-CV error assumptions were  
 684 satisfactory. With 180 kgN/ha, the simulations were of poor quality when compared to the  
 685 measurements. In a global way, the crop season 2010-11 is known to be particularly challenging in  
 686 terms of modelling, since water deficits occurred, deeper than the ones observed in 2009-10. Although  
 687 the criteria used to evaluate the model quality encountered the validation thresholds, the temporal  
 688 evolution indicates the need for model improvement by selecting other or more parameters for  
 689 identification. It may also suggest the need to use other formalisms better adapted to take into account  
 690 water deficits.





693  
694

695 **Figure 8: Model output simulations for season 2010-11, under 180kgN/ha (left graphs) and 0 kgN/ha**  
 696 **(right graphs), and for the different error assumptions, DREAM-SLS case (upper graphs), DREAM-WLS**  
 697 **case (middle graphs) and DREAM-CV case (Lower graphs). Light grey area represents the 95%**  
 698 **uncertainty boundaries. Solid black line represents the simulations obtained with mean estimates for**  
 699 **parameters.**

700

### 701 **3.6. Residual analysis**

702 The Figure 9 shows the error analysis results for the residuals between measurements and the  
 703 fitted models using the SLS, WLS and CV likelihood functions for the four cultural cycles (CS 1 to 4).  
 704 Three aspects are considered: (i) the residuals versus the simulated biomass, (ii) the comparison of  
 705 assumed and observed pdf and (iii) the partial autocorrelation coefficients of residuals.

706 In the DREAM-SLS case, the distribution of residual errors against simulated biomass  
 707 appeared quite stationary, suggesting homoscedasticity. Although the number of measurements was  
 708 low, the error histogram did not seem inconsistent with the assumed Gaussian pdf. Finally, errors were  
 709 not correlated whatever the lag, highlighting the independence of the measurements. The assumptions  
 710 for the statistical error model were thus *a posteriori* validated.

711 The error analysis graphs drawn using the DREAM-WLS or DREAM-CV approaches were  
 712 relatively close. In both cases, the residuals seemed to increase with simulated biomass, up to 10 t/ha  
 713 and were quite constant thereafter (between 10 and 20 t/ha). The residual histograms did not really  
 714 match the expected Gaussian distribution (e.g., if the histograms peaked around the zero value, there  
 715 was a dissymmetry and a tail in the positive values of residuals). Finally, the residuals were at least  
 716 significantly correlated at a lag of one measure, but in both cases this correlation was very close to the  
 717 95% boundaries.



718 In line with the graphical analysis depicted in the simulations obtained under the  
719 DREAM-WLS or DREAM-CV cases (in Figures 5 and 6), it appeared clear that the model  
720 underestimated the measurements step by step, meaning that if at a particular moment a measurement  
721 was underestimated, there would be a tendency for this to happen with the next measure. Moreover,  
722 the underestimation seemed to appear only after Julian day 520, when half the biomass had yet to be  
723 produced (for biomass superior to 10t/ha).

724 As mentioned by Wallach et al. (2006), since only a part of the between site-year variability  
725 can be predicted by crop models, correlations between model residuals often arise when several  
726 measurements are performed at different dates in a given site-year. However, this issue was  
727 acknowledged by the application of three mechanisms, respectively (i) the implementation of the  
728 experiment as a *complete randomised block distribution*, (ii) the consideration of the coefficient of  
729 variation within the error model, and finally (iii) by the implementation of a single-step sampling  
730 procedure, involving all the parameters to optimize and the variables output of the 4 cultural situation  
731 at the same time (Guillaume et al., 2011).

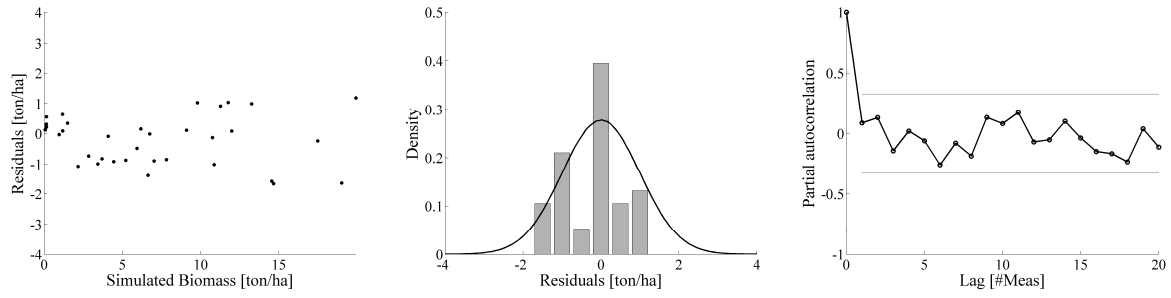
732 For these reasons, and assuming that observational climatic inputs and in-field output  
733 measurement errors were negligible, meaning, in our case, that they are due solely to genetic  
734 variability, the systematic under-estimation of the in-field biomass samples for the higher values of  
735 biomass could be fully attributed to modelling inadequacies. Rather than enabling the conclusion that  
736 could be drawn about the non-stationarity or the non-normality of the error model, it suggested the  
737 need for model improvement, whether by selecting other (or more) parameters or other formalisms  
738 (stresses effects).

739

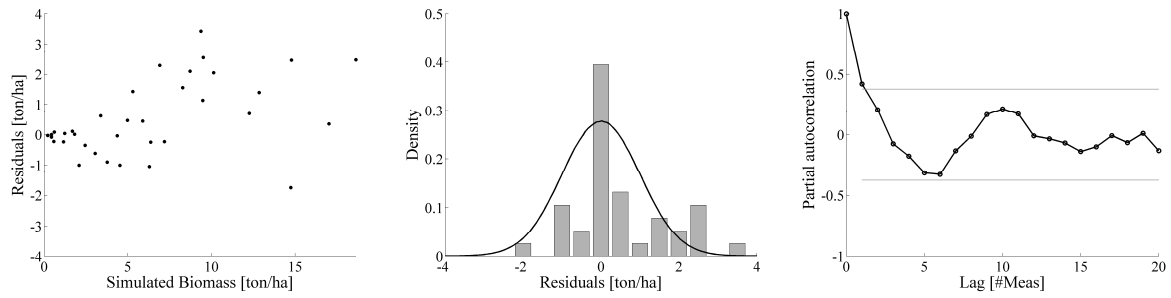
740

741

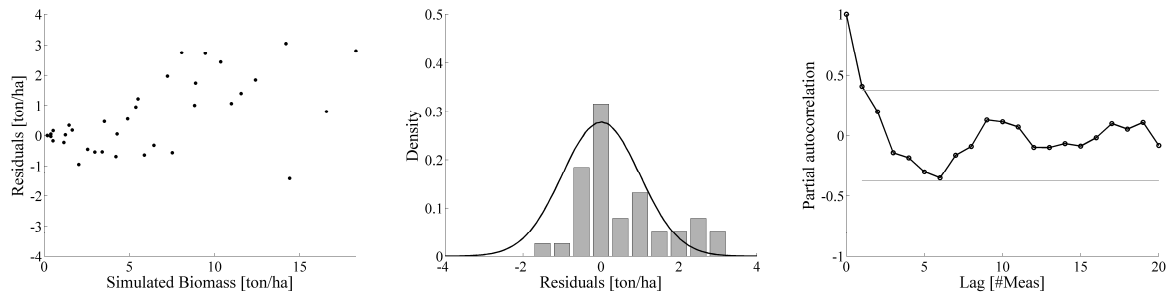
742



743



744



745

**Figure 9: Model residual analysis, for three different likelihood functions: SLS (upper graphs), WLS (middle graphs) and likelihood function for which  $CV = 0.145$  (lower graphs). Analysis of the residuals against biomass simulation (left graphs), assumed (solid black line) and observed (grey bar) pdf of residuals (centred graphs) and partial autocorrelation coefficients of residuals (solid circle black line) with 95% significance boundaries (horizontal grey line) (right graphs).**

746

747

748

749

## 750 **4. Conclusion**

751 This study assessed the potential of the DREAM algorithm for optimizing the STICS crop  
752 model parameters with the aim of improving the simulations of the biomass growth of a winter wheat  
753 culture (*Triticum aestivum* L.).

754 Nine parameters involved in leaf area development, radiation use efficiency and stress effects  
755 were chosen for optimization of the biomass growth output. Different likelihood functions and error  
756 assumptions were evaluated: a standard least square (SLS), a weighted least square (WLS) and a  
757 transformed likelihood function that makes explicit use of the coefficient of variation (CV). The  
758 performances of the DREAM algorithm were compared with a Nelder-Mead Simplex algorithm  
759 adapted to the STICS model under the OptimiSTICS package.

760 This study showed that it was possible to successfully use the DREAM algorithm combined to  
761 a complex crop model such as STICS. The DREAM algorithm offers the advantage of Bayesian  
762 techniques and MCMC simulations, i.e. the approximation of the parameters' posterior distribution,  
763 the evaluation of correlations, and the uncertainties estimation in the output predictions.

764 The parameters' sampling using the SLS likelihood function within the DREAM algorithm  
765 showed close results to those obtained using OptimiSTICS. The model evaluation criteria, RMSE, EF,  
766 and ND were substantially improved compared with the initial set of parameter values. The residual  
767 analysis also showed the validity of the SLS approach of DREAM. These results were very  
768 satisfactory and encouraging. However, when using the SLS likelihood function, considering the  
769 temporal evolution of the simulated biomass during a crop cycle characterised by significant water  
770 deficit that occurred at the early season, it appeared that the simulations did not fully respect the  
771 biophysical behaviour of plant growth which compensated later the biomass growth thanks to higher  
772 efficiency of radiation use. Insignificant or unrealistic values occurred thus for some parameters. This  
773 was probably due to the fact that too limited information was included in the dataset to efficiently  
774 sample the posterior distribution of the selected nine parameters. Although parameters with low  
775 interaction were chosen, correlation appeared in the parameters' posterior distribution. This  
776 observation highlighted the importance of adapting the experimental design to the plant-soil system

777 dynamics with modeling purposes.

778           Finally, it is worth mentioning that the proposed likelihood function based on an explicit  
779 formulation of the CV presented several advantages. The results were very close to those obtained  
780 with the standard WLS likelihood function and were satisfactory in terms of evaluation criteria,  
781 RMSE, EF and ND. From a biophysical point of view, relevant values for all parameters were  
782 obtained. Furthermore, the proposed CV likelihood function allows taking into account not only the  
783 noise on measurements but also the heteroscedasticity regularly encountered in crop modeling.

784 **Acknowledgements**

785 The authors would like to thank the SPW (D GARNE) for its financial support for the project entitled  
786 *‘Suivi en temps réel de l’environnement d’une parcelle agricole par un réseau de microcapteurs en*  
787 *vue d’optimiser l’apport en engrais azotés’.*

788 They would also like to thank the OptimISTICS team that allowed them to use the Matlab running  
789 code of the STICS model.

790 And finally they wish to thank Jasper Vrugt for his precious advices that greatly improved the quality  
791 of the present paper and for the interesting discussions about the DREAM and DREAM-ZS algorithm  
792 options.

793 We also wish to thank the two anonymous reviewers for their helpful comments.

794

795 **5. References**

- 796 Basso, B., Ritchie, J.T., 2005. Impact of animal manure, compost and inorganic fertilizer on nitrate  
797 leaching and yield in a six-year maize alfalfa rotation. *Agri. Ecosys. Environ.* 108, 329-341.
- 798 Basso B., Cammarano D., Troccoli A, Chen D., Ritchie J.T., 2010. Long-term wheat response to  
799 nitrogen in a rainfed Mediterranean environment: Field data and simulation analysis. *Eur. J. Agron.*,  
800 33, 132-138
- 801 Beaudoin N., Launay M., Sauboua E., Ponsardin G, Mary B., 2008. Evaluation of the soil crop model  
802 STICS over 8 years against the ‘on farm’ database of Bruyères catchment. *Eur. J. Agron.*, 29, 46-57.
- 803 Bechini, L., Bocchi, S., Maggiore, T., Confalonieri, R., 2006. Parameterization of a crop growth and  
804 development simulation model at sub model component level. An example for winter wheat (*Triticum*  
805 *aestivum* L.). *Environ. Model. Softw.* 21, 1042-1054.
- 806 Beven, K., 1989. Changing ideas in hydrology. The case of physically based models. *J. Hydrol.* 105,  
807 157-172.
- 808 Beven, K., 2008. Comment on “Equifinality of formal (DREAM) and informal (GLUE) Bayesian  
809 approaches in hydrologic modeling?” by Vrugt JA, ter Braak CJF, Gupta HV, Robinson BA (2008).  
810 *Stoch. Environ. Res. Risk Assess.*
- 811 Beven, K., Binley, A., 1992. The future of distributed models: Model calibration and uncertainty  
812 prediction. *Hydrol. Process.* 6, 279-298.
- 813 Beven, K., Smith, P., Freer, J., 2008. So just why would a modeller choose to be incoherent? *J.*  
814 *Hydrol.*, 354, 15-32.
- 815 Box, G, Cox, D., 1964. An analysis of transformations. *Journal of the Royal Statistical Society, Series*  
816 *B* 26(2), 211-252.
- 817 Box, G, Tiao, G, 1973. *Bayesian inference in statistical analysis.* Addison-Wesley, Reading, PA.
- 818 Brisson, N., Mary, B., Ripoche, D., Jeuffroy, M.-H., Ruget, F., Nicoulaud, B., Gate, P., Devienne-  
819 Barret, F., Antonioletti, R., Durr, C., Richard, G, Beaudoin, N., Recous, S., Tayot, X., Plenet, D.,  
820 Cellier, P., Machet, J.-M., 1998. STICS: a generic model for the simulation of crops and their water  
821 and nitrogen balances. Theory and parameterization applied to wheat and corn. *Agron.* 18, 311-346.
- 822 Brisson N., Ruget F, Gate P, Lorgeau J., Nicoulaud B., Tayo X., Plenet D., Jeuffroy M.H., Bouthier  
823 A., Ripoche D., Mary B., Justes E., 2002. STICS: a generic model for simulating crops and their water  
824 and nitrogen balances. II. Model validation for wheat and maize. *Agron.*, 22, 69-82.
- 825 Brisson, N., Gara, C., Justes, E., Roche, R., Mary, B., Ripoche, D., Zimmer, D., Sierra, J., Bertuzzi, P.,  
826 Burger, P., Bussièrè, F., Cabidoche, Y.M., Cellier, P., Debaeke, P., Gaudillère, J.P., Hénault, C.,  
827 Maraux, F., Seguin, B., Sinoquet, H., 2003. An overview of the crop model STICS. *Eur. J. Agron.* 18,  
828 309-332.
- 829 Brisson, N., Launay, M., Mary, B., Beaudoin, N., 2009. Conceptual basis, formalisations and  
830 parameterization of the STICS crop model. Editions Quae, Collection Update Sciences and  
831 Technologies, p. 297.

- 832 Brooks, S.P., 1998. Markov chain Monte Carlo and its application, *The Statistician*. J. Royal Statist.  
833 Soc. Series D.
- 834 Campolongo, F., Cariboni, J., Saltelli, A., 2007. An effective screening design for sensitivity analysis  
835 of large models. *Environ. Model. Softw.* 22, 1509-1518.
- 836 Confalonieri, R., Bechini, L., 2004. A preliminary evaluation of the simulation model CropSyst for  
837 alfalfa. *Eur. J. Agron.* 21, 223-237.
- 838 Dietzel, A., Reichert, P., 2012. Calibration of computationally demanding and structurally uncertain  
839 models with an application to a lake water quality model. *Environ. Model. Softw.* 38(0) 129-146.
- 840 Flenet, F., Villon, P., Ruget, F., 2004. Methodology of adaptation of the STICS model to a new crop:  
841 spring linseed (*Linum usitatissimum*, L.). *Agron.* 24, 367-381.
- 842 Gelman, A., Carlin, J.B., Stren, H.S., Rubin, D.B., 1997. *Bayesian Data Analysis*. Chapman and Hall,  
843 London, p. 526.
- 844 Gilks, W.R., Richardson, S., Spiegelhalter, D.J., 1996. Introducing Markov Chain Monte Carlo, in  
845 *Markov Chain Monte Carlo in Practice*: Chapman & Hall, London, pp. 1-19.
- 846 Guillaume, S., Bergez, J.E., Wallach, D., Justes, E., 2011. Methodological comparison of calibration  
847 procedures for durum wheat parameters in the STICS model. *Eur. J. Agron.* 35, 115-126
- 848 Hansen, S., Jensen, H., Nielsen, N., Swenden, H., 1990. DAISY – Soil Plant Atmosphere System  
849 Model S NP0 Research, in the NAEP report, The Royal Veterinary and Agricultural University, Nr  
850 A10.
- 851 Hastings, W.K., 1970. Monte Carlo sampling methods using Markov chains and their applications.  
852 *Biometrika* 57, 97-109.
- 853 Jansen, M., Hagenars, T., 2004. Calibration in a Bayesian modelling framework, In: van Boekel,  
854 M.A.J.S., Stein, A., van Bruggen, A.H.C. (Ed.), *Bayesian Statistics and Quality Modelling in the Agro-  
855 food Production Chain*: Kluwer Academic, Dordrecht.
- 856 Jeremiah, E., Sisson, S.A., Sharma, A., Marshall, L., 2012. Efficient hydrological model parameter  
857 optimization with Sequential Monte Carlo sampling. *Environ. Model. Softw.* 38(0) 283-295.
- 858 Joseph, J.F., Guillaume, J.H.A., 2013. Using a parallelized MCMC algorithm in R to identify  
859 appropriate likelihood functions for SWAT. *Environ. Model. Softw.* 46(0) 292-298.
- 860 Laloy, E., Fasbender, D., Bielders, C.L., 2010. Parameter optimization and uncertainty analysis for  
861 plot-scale continuous modeling of runoff using a formal Bayesian approach. *J. Hydrol.* 380, 82-93.
- 862 Laloy, E., Vrugt, J.A., High-dimensional posterior exploration of hydrologic models using multiple-try  
863 DREAM\_(ZS) and high-performance computing, *Water Resources Research*, 48, W01526,  
864 doi:10.1029/2011WR010608, 2012.
- 865 Lamboni, M., Makowski, D., Lehuger, S., Gabrielle, B., Monod, H., 2009. Multivariate global  
866 sensitivity analysis for dynamic crop models. *Field Crop. Res.* 113, 312–320.
- 867 Launay, M., Flenet, F., Ruget, F., Garcia de Cortazar Atauri, I., 2005. Généricité et méthodologie  
868 d'adaptation de STICS à de nouvelles cultures. *Séminaire STICS, Carry-le-Rouet*, 55-57 p.
- 869 Loague, K., Green, R.E., 1991. Statistical and graphical method for evaluating solute transport models:

- 870 overview and application. *J. Contam. Hydrol.* 7, 51-73.
- 871 Makowski, D., Wallach, D., Tremblay, M., 2002. Using a Bayesian approach to parameter estimation;  
872 comparison of the GLUE and MCMC methods. *Agron.* 22, 191-203.
- 873 Makowski, D., Naud, C., Jeuffroy, M.H., Barbottin, A., Monod, H., 2006. Global sensitivity analysis  
874 for calculating the contribution of genetic parameters to the variance of crop model prediction. *Reliab.*  
875 *Eng. Sys. Saf.* 91(10), 1142-1147.
- 876 Mansouri, M., Dumont, B., Destain, M.-F., 2013. Modeling and prediction of nonlinear environmental  
877 system using Bayesian methods. *Computers and Electronics in Agriculture* 92(0) 16-31.
- 878 Metropolis, N., Rosenbluth, A., Rosenbluth, M., Teller, A., Teller, E., 1953. Equation of state  
879 calculations by fast computing machines. *J. Chem. Phys.* 21, 1087-1092.
- 880 Minunno, F., van Oijen, M., Cameron, D.R., Cerasoli, S., Pereira, J.S., Tomé, M., 2013. Using a  
881 Bayesian framework and global sensitivity analysis to identify strengths and weaknesses of two  
882 process-based models differing in representation of autotrophic respiration. *Environ. Model. Softw.*  
883 42(0) 99-115.
- 884 Monod, H., Naud, C., Makowski, D., 2006. Uncertainty and sensitivity analysis for crop  
885 models. *In: Wallach, D., Makowski, D., Jones, J. W. (eds.) Working with Dynamic Crop Models:  
886 Evaluation, Analysis, Parameterization, and Applications*, Chapter 4. Elsevier, pp. 55-100.
- 887 Monteith, J., 1996. The quest for balance in crop modeling. *Agron. J.* 88, 695-697.
- 888 Preece, D., 1990. R.A. Fisher and experimental design : a review. *Biometrics*, 46(4), 925-935.
- 889 Rasmussen, R., Hamilton, G., 2012. An approximate Bayesian computation approach for estimating  
890 parameters of complex environmental processes in a cellular automata *Environ. Model. Softw.* 29(1)  
891 1-10.
- 892 Ritchie, J.T., Otter, S., 1984. Description and performance of CERES-Wheat, a user-oriented wheat  
893 yield model. *USDA-ARS-SR Grassland Soil and Water Research Laboratory Temple TX*, 159-175.
- 894 Ruget F., Brisson N., Delécolle R., Faivre R., 2002. Sensitivity analysis of a crop simulation (STICS)  
895 in order to determine accuracy needed for parameters. *Agron.*, 22:133-158.
- 896 Schoups, G. and Vrugt, J., 2010. A formal likelihood function for parameter and predictive inference of  
897 hydrologic models with correlated, heteroscedastic, and non-Gaussian errors. *Water Resour. Res.*, 46,  
898 W10531, doi:10.1029/2009WR008933
- 899 Singh, A., Tripathy, R., Chopra, U., 2008. Evaluation of CERES-Wheat and CropSyst models for  
900 water–nitrogen interactions in wheat crop. *Agric. Water Manag.* 95, 776-786.
- 901 Ter Braak, C., 2006. A Markov chain Monte Carlo version of the genetic algorithm differential  
902 evolution: Easy Bayesian computing for real parameter spaces. *Stat. Comput.* 16, 239-249.
- 903 Tremblay, M., Wallach, D., 2004. Comparison of parameter estimation methods for crop models.  
904 *Agron.* 24, 351-365.
- 905 Van Diepen, C., Wolf, J., Van Keulen, H., Rappoldt, C., 1989. WOFOST: a simulation model of crop  
906 production. *Soil Use Manag.* 5, 16-24.
- 907 Varella, H., 2011. Inversion d'un modèle de culture pour estimer spatialement les propriétés des sols et



- 908 améliorer la prédiction de variables agro-environnementales. PhD thesis. 207 pp, Univ of Avignon.
- 909 Varella, H., Guérif, M., Buis, S., 2010a. Global sensitivity analysis measures the quality of parameter  
910 estimation: the case of soil parameters and a crop model. *Environ. Model. Softw.* 25, 310–319.
- 911 Varella, H., Guérif, M., Buis, S., Beaudoin, N., 2010b. Soil properties estimation by inversion of a  
912 crop model and observations on crops improves the prediction of agro-environmental variables. *Eur. J.*  
913 *Agron.* 33(2), 139-147.
- 914 Vrugt, J., Gupta, V., Bouten, W., Sorooshian, S., 2003. A shuffled Complex Evolution Metropolis  
915 algorithm for optimisation and uncertainty assessment of hydrologic model parameters. *Water*  
916 *Ressour. Res.* 39(8), 1201.
- 917 Vrugt, J.A., Gupta, H.V., Nualláin, B., Bouten, W., 2006. Real-Time Data Assimilation for Operational  
918 Ensemble Streamflow Forecasting. *J. Hydrometeor.* 7(3) 548-565.
- 919 Vrugt, J., ter Braak, C., Clark, M., Hyman, J., Robinson, B., 2008a. Treatment of input uncertainty in  
920 hydrologic modeling using adaptive Markov Chain Monte Carlo sampling. *Water Ressour. Res.* 44.
- 921 Vrugt, J., ter Braak, C., Gupta, H., Robinson, B., 2008b. Response to comment by Keith Beven on  
922 ‘Equifinality of formal (DREAM) and informal (GLUE) Bayesian approaches in hydrologic  
923 modeling?’ *Stoch. Environ. Res. Risk Assess.*, 23, 7p.
- 924 Vrugt, J., ter Braak, C., Diks, C., Robinson, B., Hyman, J., Higdon, D., 2009a. Accelerating Markov  
925 chain Monte Carlo simulation by self adaptive differential evolution with randomized subspace  
926 sampling. *Int. J. Nonlinear Sci. Numer. Simul.* 10, 271–288.
- 927 Vrugt, J., ter Braak, C., Gupta, H., Robinson, B., 2009b. Equifinality of formal (DREAM) and  
928 informal (GLUE) Bayesian approaches in hydrologic modeling. *Stoch. Environ. Res. Risk Assess.*, 23,  
929 7 p.
- 930 Vrugt, J.A., Laloy, E., and ter Braak, C.J.F., Differential Evolution Adaptive Metropolis with  
931 Sampling from past states, *SIAM journal on Optimization*, In Review, 2011
- 932 Wallach, D., Goffinet, B., Bergez, J.-E., Debaeke, P., Leenhardt, D., Aubertot, J.-N., 2001. Parameter  
933 estimation for crop models: A new approach and application to a corn model. *Agron. J.* 93(4), 757-  
934 766.
- 935 Wallach, D., Buis, S., Lechapentier, P., Bourges, J., Clastre, P., Launay, M., Bergez, J.E., Gueriff, M.,  
936 Soudais, J., Justes, E., 2011. A package of parameter estimation methods and implementation for the  
937 STICS crop-soil model. *Environ. Model. Softw.* 26, 386-394.
- 938 Wallach, D., Makowski, D., Jones, J., 2006. Working with Dynamic Crop Models: Evaluation,  
939 Analysis, Parameterization and Applications. Wallach D., Makowski D., Jones J., Elsevier, Amsterdam  
940 (Ed).
- 941 Wallach, D., Van Evert, F., Adam, M., 2009. Parameter estimation software for crop models.  
942 Proceedings of the AgSAP Conference 2009: Egmond aan Zee, The Netherlands, pp. 342-343.
- 943 Williams, J.R., Jones, C.A., Kiniry, J.R., Spanel, D.A., 1989. The EPIC crop growth model. *Trans.*  
944 *ASAE* 32, 497-511.
- 945 Wösten, J.H.M., Lilly, A., Nemes, A., Le Bas, C., 1999. Development and use of a database of

- 946 hydraulic properties of European soils. *Geoderma* 90, 169–185.
- 947 Wu, Y., Liu, S., 2012. Automating calibration, sensitivity and uncertainty analysis of complex models  
948 using the R package Flexible Modeling Environment (FME): SWAT as an example. *Environ. Model.*  
949 *Softw.* 31(0) 99-109.
- 950